

# **Stony Brook University**



OFFICIAL COPY

**The official electronic file of this thesis or dissertation is maintained by the University Libraries on behalf of The Graduate School at Stony Brook University.**

**© All Rights Reserved by Author.**

# **Nanostructured Hydrogel Implants for Post Lumpectomy Patients**

A Thesis Presented

by

**Mahati Elluru**

to

The Graduate School

in Partial Fulfillment of the

Requirements

for the Degree of

**Master of Science**

in

**Chemistry**

Stony Brook University

**May 2011**

**Stony Brook University**

The Graduate School

**Mahati Elluru**

We, the thesis committee for the above candidate for the  
Master of Science degree, hereby recommend  
acceptance of this thesis.

**Dr. Benjamin Chu, Advisor**  
**Distinguished Professor, Chemistry Department**

**Dr. Benjamin Hsiao, Advisor**  
**Professor and Chair, Chemistry Department**

**Dr. Robert B. Grubbs, Chairman of Thesis Committee**  
**Associate Professor, Chemistry Department**

**Dr. Peter J. Tonge**  
**Professor, Chemistry Department**

This thesis is accepted by the Graduate School

Lawrence Martin  
Dean of the Graduate School

Abstract of the Thesis

**Nanostructured Hydrogel Implants for Post Lumpectomy Patients**

by

**Mahati Elluru**

**Master of Science**

in

**Chemistry**

Stony Brook University

**2011**

Breast cancer patients encounter several complications while undergoing the lumpectomy procedure. Modified Pluronics possessing the ability to crosslink can function as implants for post lumpectomy patients. In this project, the tri-block copolymer, Pluronic F127, a member of the Pluronics copolymers, has been chemically modified by introducing vinyl groups at the terminal ends of the polymer chain. The modified copolymer is cross-linkable by UV irradiation and forms a soft, tough gel with mechanical properties comparable to native human breast tissue. The polymer can be engineered to replicate the physical and mechanical properties of the human breast tissue. This can be done by varying the block length and block ratio as well as the extent of cross-linking, which can be achieved by altering the irradiation time, the polymer concentration and the concentration of the photo-initiator. The gel possesses both hydrophilic and hydrophobic domains that can be utilized to incorporate additional agents as required. The constituents of the gel and the cross-linked gel have been tested for cytotoxicity with the preadipocyte cell line. With the incorporation of growth factors and other proteins, the cross-

linked Pluronics have a potential to be used as a scaffold for regeneration of the native breast tissue while undergoing *in vivo* degradation.

# Table of Contents

<b>List of Figures</b> .....	vii
<b>Acknowledgements</b> .....	viii
<b>Chapter 1 Introduction and Background</b> .....	1
1.1 Breast Conservation Surgery.....	2
1.2 Current Breast Reconstruction Techniques.....	2
1.3 Hydrogels .....	4
1.4 Pluronics.....	5
1.4.1 Properties .....	6
1.4.2 Pluronic F-127.....	9
<b>Chapter 2 Research Objectives</b> .....	11
<b>Chapter 3 Experimental Section</b> .....	14
3.1 Materials.....	14
3.2 Chemical Modification of Pluronic F-127 .....	15
3.3 Gel Composition and Preparation.....	15
3.4 Gamma Irradiation.....	16
3.5 UV Radiation Induced Photo Cross-linking.....	17
3.6 Swelling Studies .....	17
3.7 Storage Modulus.....	18
3.8 Cell Studies .....	18
3.8.1 MTS Assay .....	24
3.8.2 Live/Dead Assay .....	25
3.8.3 Photo-initiator cytotoxicity .....	26
3.8.4 Cell studies with cross-linked gel .....	27
3.9 Sodium Acrylate Cross-linking .....	28
3.10 Scanning Electron Microscopy.....	28
3.11 Small Angle X-ray Scattering .....	29
<b>Chapter 4 Results and Discussion</b> .....	<b>30</b>

4.1 Chemical Modification of Pluronics .....	30
4.2 Gamma Radiation .....	32
4.3 UV Radiation Induced Photo Cross-linking.....	33
4.4 Swelling Studies .....	36
4.5 Storage Modulus.....	37
4.6 Cell Studies .....	38
4.6.1 MTS Assay .....	39
4.6.2 Live – Dead Assay .....	41
4.6.3 Photo-initiator cytotoxicity.....	43
4.6.4 Cell studies with cross-linked gel .....	44
4.7 Sodium Acrylate Cross-linking .....	45
4.8 Scanning Electron Microscopy.....	47
4.9. Small Angle X-ray Scattering .....	49
<b>Chapter 5 Conclusion and Future Work.....</b>	<b>52</b>
5.1 Formation of porous network.....	52
5.2 Structural Studies.....	54
5.3 Modification of Surface Properties for Cell Adhesion .....	55
5.4 Conclusion.....	56
<b>Bibliography .....</b>	<b>57</b>

# List of Figures

Figure 1.1: Pluronics block copolymer molecule,.....	6
Figure 1.2: Schematic representation of aggregation structures formed by block copolymers in solution: (A) copolymer unimer; (B) spherical micelle in a solvent selective for the end-blocks; (C) and (D) gel-like micro-structures formed by micelles in the ‘gel’ phase <sup>13</sup> .....	7
Figure 1.3: (A) Polymer chains, (B) Micellar phase, (C) ‘Gel’ phase.....	7
Figure 1.4: Micellization and gelation of Pluronics; .....	8
Figure 1.5: Schematic phase diagram for the phase behavior of amphiphilic EPE tri-block copolymers in aqueous solution <sup>22</sup> .....	9
Figure 1.6: Pluronics F-127 .....	9
Figure 3.1: Esterification reaction of Pluronic F127 with acryloyl chloride .....	15
Figure 3.2: UV irradiation of Diacrylated-F127 .....	17
Figure 3.3: Cell counting using Haemocytometer <sup>29</sup> .....	23
Figure 3.4: Irgacure 2959.....	26
Figure 4.1: <sup>1</sup> H-NMR Spectrum of Pluronic F-127 .....	31
Figure 4.2: <sup>1</sup> H-NMR Spectrum of Diacrylated F-127 (Inset: 5-7 ppm portion of spectrum).....	32
Figure 4.3: UV radiation induced photo-polymerization reaction <sup>25</sup> .....	34
Figure 4.4: Formation of cross-linked DA-F127 polymer network (A) DA-F127 gel, (B) UV irradiation, (C) Cross-linked hydrogel, (D) Cross-linked polymer disk.....	36
Figure 4.5: Swelling study, (A) Swelling ratio, (B) Change in gel volume.....	37
Figure 4.6: Change in storage modulus of cross-linked DA-F127 during swelling .....	38
Figure 4.7: MTS Assay of A: Cells, B: DA-F127 gel .....	40
Figure 4.8: Live Dead assay images, (A) Control, (B) 30%w/w DA-F127 gel;                      green dots: live cells, red dots: dead cells .....	42
Figure 4.9: Photo-initiator cytotoxicity from Trypan Blue staining.....	43
Figure 4.10: (A),(B) Gel sample with cells, (C) Cells adjacent to gel (gel is pink) .....	45
Figure 4.11: Viscosity of 30%w/w 2:1 F-127: Sodium Acrylate gel before and after UV irradiation; Initial: before UV radiation, 0 hour: after UV radiation .....	47
Figure 4.12: SEM images of cross-linked DA-F127 gel cross-section .....	48
Figure 4.13 (A) Typical SAXS intensity pattern of (S1) 30% w/w 2:1 DA-F127: PEG (1.5 kDa), (S2)20% w/w DA-F127, (S3) 30% w/w DA-F127. (B) Corresponding radially averaged 1-D intensity profile.....	49
Figure 4.14: Integrated fitting curves of S1, S2 and S3.....	50



# Acknowledgements

I would like to express my sincere gratitude to my advisors, Prof. Benjamin Chu and Prof. Benjamin Hsiao for their continuous support, motivation and enthusiasm throughout my research. I could not have imagined having better advisor and mentor for my study at Stony Brook University. I would like to thank Prof. Michael Hadjiargyrou for guiding me and providing me the opportunity to conduct biological testing. In addition, I would like to thank all my committee members for their time and valuable suggestions.

I am thankful to Dr. Chirakkal Krishnan, Dr. Jonathan Chiu and Dr. Hongyang Ma, who I believe were the best mentors I could have for guiding me in various aspects of my research for the past two years. Si Hui Guan, Karin Wang and all my other colleagues were always willing to help me in my research and give their best suggestions. It would have been a lonely lab without them. I would also like to thank Jane Wainio and Dr. Dufei Fang for their support during my research.

I would like to thank my parents and my brother for being supportive of all my decisions and for always being there to share my excitements and disappointments in graduate life. I cannot thank my friend, Shraddha Surve, enough for her encouraging talks, constructive criticism and praises, genuine caring and many other things. I would also like to thank all my friends, my cousins and my family in the United States, for being a major part of my life during graduate school. They have made my experience very enjoyable and memorable, and made Stony Brook feel like home.

# Chapter 1

## Introduction and Background

This thesis describes the initial stages of development of a novel polymer-based hydrogel, intended for use as implants for post lumpectomy patients. The first half of this chapter gives a brief history and background of the current breast reconstruction techniques; the second half provides an introduction to hydrogels and the specific polymers used in this study.

Radical mastectomy, introduced by William Halsted over 100 years ago was the treatment of choice for breast cancer of any size, regardless of the age of a patient. The likelihood of conducting a surgical procedure that would conserve the breast tissue was not widely considered until the latter half of the 20<sup>th</sup> century. It was then that a better understanding of the biological processes underlying breast cancer began to develop. Randomized clinical trials were conducted to compare the long term survival rates of patients treated by extensive surgery, with those who were treated by conservative surgery, in conjunction with post operative radiation therapy. Results from these trials indicated equivalent overall survival rate. In 1990, a consensus panel of the National Institutes of Health (NIH) concluded that, ‘breast conservation, defined as the excision of the tumor and surrounding tissue, with axillary dissection, followed by radiation therapy, was preferable to mastectomy for the majority of women with stage I or II breast cancer.’<sup>1,2</sup>

## **1.1 Breast Conservation Surgery**

Breast conservation surgery (BCS) is now a widely accepted form of treatment in patients with early stages of breast cancer. This surgery is usually followed by radiation therapy to reduce the risk of local recurrences.<sup>3</sup> BCS is thus, a process that involves the removal of lump or tumor from the infected breast and is often considered to result in a minimal deformation of the breast. BCS is also known as ‘Lumpectomy’ implying the removal of only the lump or tumor, thus conserving the remaining tissue. Mastectomy, on the other hand, is a surgical procedure that involves the removal of the entire breast tissue affected by the tumor.

Breast conservation surgery often deforms the shape of the breast tissue and several patients have been observed to report post operative breast asymmetry. Many BCS patients require multiple excisions of their tumor along with radiation therapy, which usually results in poor esthetic appearance.<sup>4</sup> Owing to the large number of clinical occurrences of breast cancer, breast reconstruction, following lumpectomy or mastectomy, has become one of the most common reconstructive procedures performed in the United States.<sup>5</sup>

## **1.2 Current Breast Reconstruction Techniques**

Post-surgery breast reconstruction is an option chosen by most women. With known psychological benefits, breast reconstruction has become a significant part of breast cancer management. With increased anatomic knowledge of the breast tissue, several techniques for

breast reconstruction have been studied and explored. Reconstruction using autologous tissue was one of the earliest explored options for breast reconstruction. Early attempts with autologous techniques were unsuccessful, not reproducible and also resulted in significant donor-site morbidity. These failures led to the development of an array of prosthetic options.

Reconstruction by injecting filler substances into the breast cavity was one of the explored breast reconstruction strategies. Filler substances included petroleum jelly, paraffin, ground rubber, polyester fabrics etc. However, these injections resulted in several complications such as pulmonary emboli, skin necrosis and the formation of granulomas and fistulas. Introduction of silicone implants in 1960s revolutionized the field of mammoplasty. Silicone breast prosthesis gained popularity and an estimated one million women received silicone implant breast as a part of reconstruction following surgery for breast cancer or prophylactic mastectomy between 1963 and 1988. Over time, there have been modifications to these prostheses with respect to shapes, textures and consistencies.<sup>6,7</sup> However, these implants were later surrounded with several safety concerns and were linked to a variety of illnesses including connective-tissue diseases and rheumatic disorders.<sup>8</sup> These safety concerns led to the development of saline filled implants as an alternative. Saline filled implants were associated with the problem of rippling and an increased risk of rupture, though not harmful.<sup>6</sup>

There have been advances and improvements in both autologous techniques and the quality of prosthetic options. However, autologous techniques are very complex, involve long and complicated procedures and are very expensive. Prosthetic options, though simpler and cheaper, have their own specific disadvantages.<sup>7</sup>

Mastectomy patients have the option of choosing between autologous techniques or prosthetic options for breast reconstruction. However, post lumpectomy patients can only decide on autologous procedures since prosthetic implants are not available for cavities formed after lumpectomy. The breast cavities formed after breast conservation surgeries are of various shapes and sizes depending on the shape and size of the tumors. It is not practical and not possible to create customized prosthetic implants for each patient. Prosthetic implants are also known to pose difficulties with post-operative imaging techniques.

Currently, several tissue engineering strategies are being explored. Use of these strategies could result in autologous breast reconstruction without a donor site and its related morbidity.

## **1.3 Hydrogels**

Hydrogels are three dimensional networks of polymer chains that are hydrophilic and are capable of imbibing large amounts of water or biological fluids. These networks consist of homo-polymers or copolymers and can be swollen by water but cannot be dissolved in it, due to the presence of cross-links. The swollen networks possess both the cohesive properties of solids and the diffusive transport characteristics of liquids. Hydrogels have a variety of medical and pharmaceutical applications, such as drug delivery, tissue engineering, regenerative medicine etc. As a result of their high water content and soft consistency, they are the closest resemblance to natural living tissue than any other class of synthetic biomaterials.<sup>9,10</sup>

Hydrogels may be chemically stable or they may degrade and ultimately disintegrate and dissolve. These gels are called ‘reversible’ or ‘physical’ gels when the networks are held together

by molecular entanglements, or secondary forces, such as ionic, hydrogen bonding or hydrophobic forces. Physical hydrogels are often not homogeneous, since clusters of molecular entanglements, or hydrophobic or ionic domains can create inhomogeneities. Hydrogels are called ‘permanent’ or ‘chemical’ gels when they are covalently cross-linked networks. Chemical hydrogels can be generated by cross-linking of water soluble polymers. Similar to physical hydrogels, chemical hydrogels are mostly not homogeneous. They may contain regions of low water swelling and high cross-linking density, called ‘clusters’, that are dispersed within regions of high swelling and low cross-linking density.<sup>11</sup>

## 1.4 Pluronics

Pluronics block copolymers, also known as ‘ploxamers’, consist of ethylene oxide (EO) and propylene oxide (PO) blocks arranged in a basic X-Y-X structure (Figure 1.1). They are a family of symmetric tri-block copolymers with a central block of hydrophobic poly (propylene oxide) (PPO) sandwiched between blocks of hydrophilic poly (ethylene oxide) (PEO). This arrangement results in an amphiphilic copolymer. Owing to their amphiphilic properties, these copolymers exist in aqueous solutions in the form of single chains, micelles or physical gels. Pluronics polymers have widespread industrial and biomedical applications in their uses as emulsifying, wetting, thickening, coating, solubilizing, stabilizing, dispersing, lubricating, and foaming agents.<sup>12</sup>

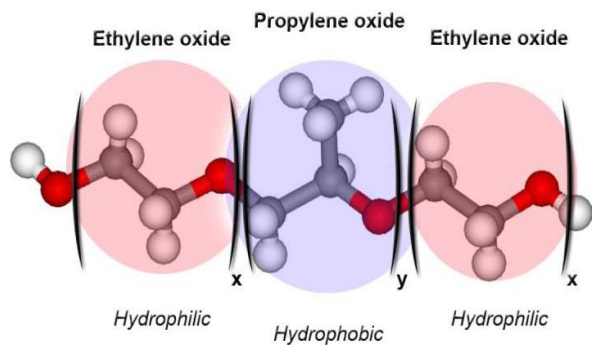


Figure 1.1: Pluronic block copolymer molecule, x: number of PEO groups; y: number of PPO groups<sup>13</sup>

### 1.4.1 Properties

An important property of amphiphilic block copolymers is the ability of block copolymer molecules to self-assemble into micelles in aqueous solutions. At low solution concentrations, the polymers exist as molecular solutions in water. As the concentration increases, the difference in solubility of different copolymer blocks in the solvent leads to self-association of molecules. The less soluble blocks shrink in solution and aggregate with each other to form the micelle core while the soluble blocks form the micelle shell or corona.<sup>14</sup> Thus at concentrations above the critical micelle concentration (CMC), the copolymer molecules combine to form multi-molecular aggregates with a central hydrophobic PPO core and a hydrophilic shell consisting of PEO chains extending into the dispersing aqueous medium. This process is known as ‘micellization’. The micelles can be, for example, spherical or rod-like depending, for example, on the copolymer concentration, the ratio of EO and PO blocks and temperature.<sup>15</sup> It should be noted that the CMC may not be sharp. Micellization and micelle structure transitions can occur over a fairly broad range of concentrations.

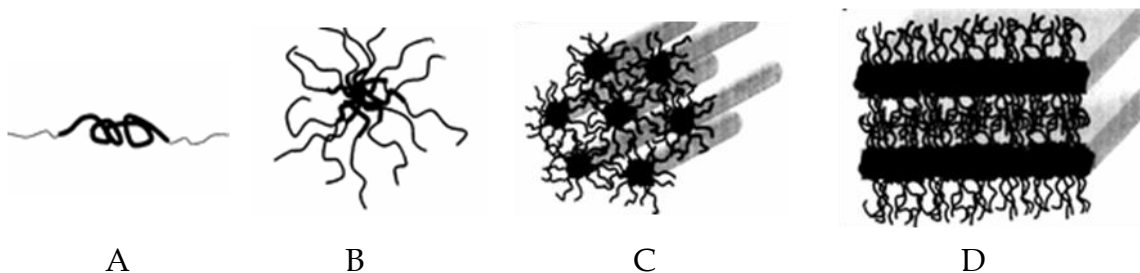


Figure 1.2: Schematic representation of aggregation structures formed by block copolymers in solution: (A) copolymer unimer; (B) spherical micelle in a solvent selective for the end-blocks; (C) and (D) gel-like micro-structures formed by micelles in the ‘gel’ phase<sup>13</sup>

In aqueous Pluronic solutions, micelle formation is also dependent on temperature. The PEO-PPO-PEO tri-block copolymer exists in the unimer state in aqueous solution at low temperatures since both blocks (PEO and PPO) are soluble at low temperatures. Increasing the temperature causes an increase in the hydrophobicity of the PPO block and leads to micelle formation. The temperature at which this transition occurs is referred to as the ‘critical micelle temperature’ (CMT).<sup>16</sup>

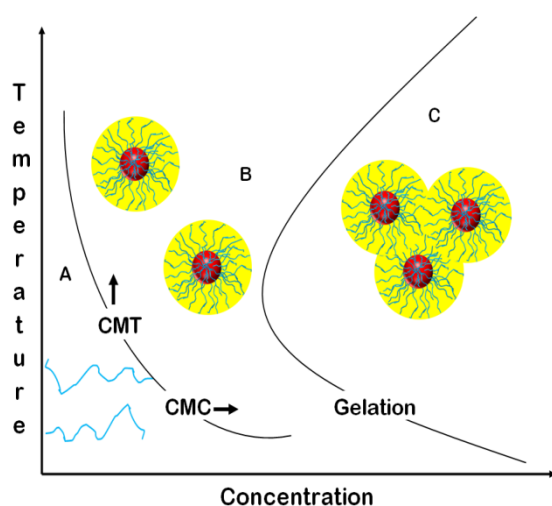


Figure 1.3: (A) Polymer chains, (B) Micellar phase, (C) ‘Gel’ phase<sup>17</sup>



At appropriate concentration and temperature, the Pluronics thus form micelles in solution. At higher polymer concentrations, the closed packing of micelles or the rearrangement of the hydrophilic and hydrophobic regions results in the formation of gel-like ordered structures. Above a certain concentration known as ‘critical gel concentration’ (CGC), the micelles overlap to yield a gel-like medium with ordered quasi-lattice packing. Thus Pluronics solutions exhibit thermally reversible gelation behavior.<sup>18,19,20</sup>

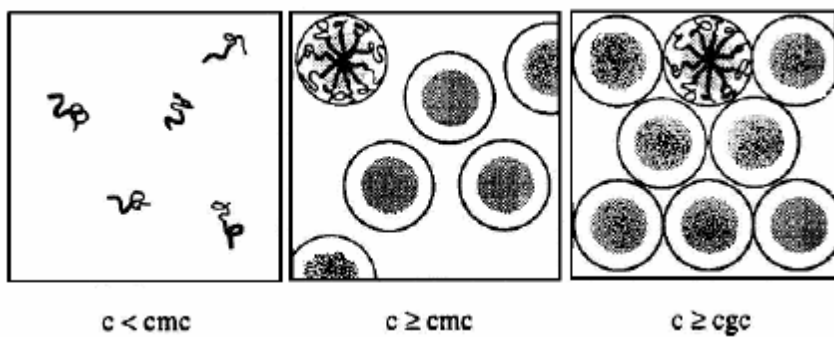


Figure 1.4: Micellization and gelation of Pluronics;  
 $c$ : concentration,  $cmc$ : critical micelle concentration,  $cgc$ : critical gel concentration<sup>19</sup>

Thus, the liquid micellar phase at low concentrations and temperature can be transformed into a physical ‘gel’ with increase in temperature.<sup>21</sup> The first gel-like structure is often a cubic structure (body centered cubic or face-centered cubic, bcc or fcc, respectively), formed by an ordered packing of spherical micelles. At higher polymer concentrations, the arrangement of the hydrophilic and hydrophobic regions leads to the formation of hexagonal or lamellar structures as shown in Figure 1.5. It is to be noted that the solubility of block co-polymers decreases with increasing temperature and, above a certain temperature, phase separation occurs. This phenomenon is known as ‘clouding’, as also shown in the figure below.<sup>22</sup>

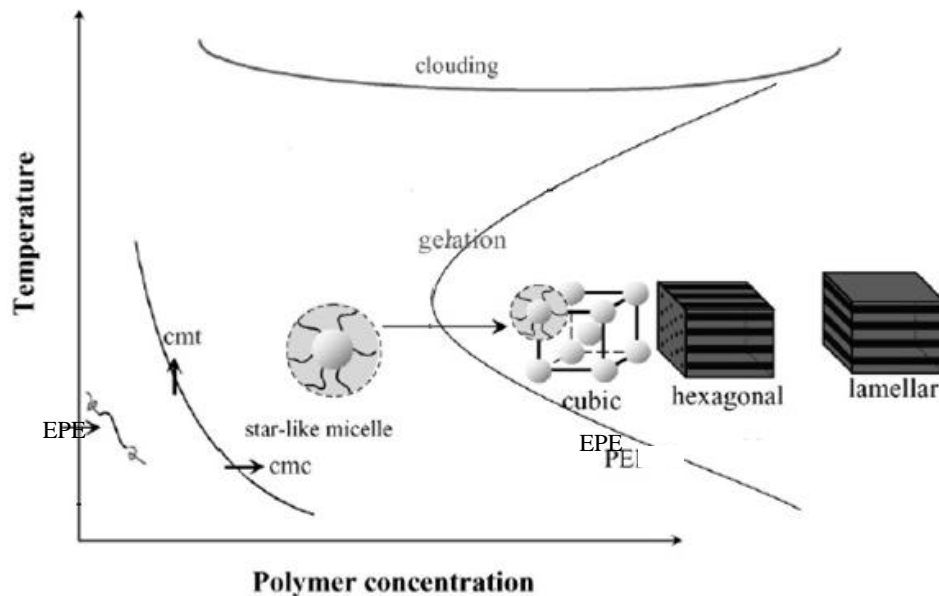


Figure 1.5: Schematic phase diagram for the phase behavior of amphiphilic EPE tri-block copolymers in aqueous solution<sup>22</sup>

## 1.4.2 Pluronic F-127

F-127 is one of the most important members in the family of Pluronic due to its excellent biocompatibility and FDA approval for use in pharmaceutical applications. It is a tri-block copolymer with the general formula  $\text{EO}_{99}\text{-PO}_{69}\text{-EO}_{99}$  and an average molecular weight of  $1.26 \times 10^4$  Daltons. It contains approximately 70% (w/w) ethylene oxide, which accounts for its hydrophilicity.<sup>13,18</sup>

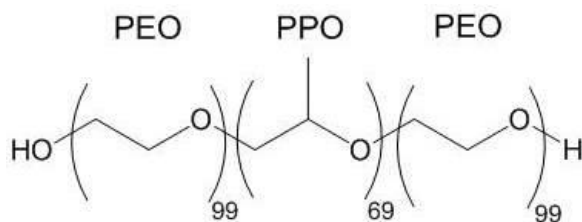


Figure 1.6: Pluronic F-127

F-127 has increased solubility in cold water in comparison to hot water due to the increased solvation and hydrogen bonding at lower temperatures for the PPO block. Aqueous solutions of 20 – 30% F-127 exhibit interesting reverse thermal gelation characteristics. They exist as liquid at refrigerated temperatures, such as 4-5 °C, but transform into a gel upon warming to room temperature. This gelation behavior is reversible.<sup>15,23</sup>

The levels of viscosity attained by Pluronic hydrogels at 37 °C are not high enough for certain clinical applications, such as for use as implants in the breast cavity. In the current application, the gel loses its structural integrity upon dilution with other aqueous fluids, due to a reduction in the copolymer concentration required for the close packing of Pluronic micelles. The hydrogels thus become very soft, can easily be disintegrated and undergo dissolution on contact with an *excess* amount of buffer solution. Consequently, the hydrogels disintegrate when diluted in the physiological environment because the copolymer concentration is being diluted below the critical gel concentration. Under these conditions, the local copolymer concentration becomes inadequate for association of polymeric micelles into closely assembled structures, thus resulting in relatively short *in vivo* residence times.<sup>24,25</sup>

# Chapter 2

## Research Objectives

In this project, we aim to develop an implant that can mimic both the physical and mechanical properties of the human breast tissue and has the required strength and softness that is ideally suited for implantation. The implant should have the following characteristics:

1. Be able to withstand the entire radiation treatment without substantial decomposition
2. Should not obscure X-ray examination on surrounding tissues
3. Should have the ability to be molded into any required shape and size
4. Should retain its shape while maintaining flexibility, and simulate the physical and mechanical properties of the natural tissues, such as glandular and adipose tissue, which are the predominant tissue components of the human breast
5. Should be biocompatible and biodegradable, with degradation profiles suitable for tissue regeneration
6. Should provide the porosity and pore size distribution for timely delivery of medication, and agents to promote cell growth.

To differentiate the current implant from previous devices, points (5) and (6) are particularly noteworthy. Consequently, the materials used for this application should be biocompatible, and more importantly, biodegradable, so that the implant can function as a scaffold for regeneration of the native tissue. This implies that it should possess many of the

properties that favor cell adhesion, penetration and regeneration with the appropriate physical and mechanical properties, as mentioned in point (6). Natural tissue should be able to develop during degradation of the implant, without any long term remainder of foreign material in the body, suggesting the need for control of biodegradation profiles and medication/growth factor release at the appropriate time. The current thesis touches some aspects of the requirements, recognizing that further work needs to be carried out in order to achieve the final goal. In addition, the material used for the implantation should be nonallergenic and nonpyrogenic. It should be aesthetically and ergonomically appealing and be economical at the same time. It needs to be stable after implantation and must be easy to use, without any complexities in the operating room. The implanted material should result in minimal immune response upon implantation and should have minimal donor-site morbidity. It cannot be over emphasized that the scaffold must possess surface characteristics suitable for cell adhesion as well as to have a high degree of porosity to enable cells to migrate into and to populate the scaffold to facilitate vascularization and structural integration with the surrounding tissue.<sup>26,27</sup>

Since no commercially viable products exist at present for lumpectomy patients, this new material, can be the pioneering product to greatly diminish the psychological impact of lumpectomies on patients and also become the key to encourage and assuage patients to receive necessary lumpectomy treatments.

## **Approach**

Hydrogels fabricated from pure unmodified Pluronics, with all its unique properties, form a physical gel at body temperature. Unfortunately, the gels so formed disintegrate in a relatively short span of time in the human body and thus will not be useful for our application.

Cross-linking of Pluronics can turn the physical gel into a covalently bonded chemical gel that cannot be easily disintegrated as a result of chemical cross links. However, this chemically cross-linked gel will no longer be completely thermo-reversible. However, there is a pathway to maintain limited thermal reversibility. Nevertheless, this approach has not been tested, in view of lack of time. The slower disappearance of partially chemical cross-linked gel can now be utilized to our advantage because the composite polymer network now has a potential to act as scaffold for natural regeneration of the tissue.

# Chapter 3

## Experimental Section

### 3.1 Materials

Pluronic F-127 [(PEO)<sub>99</sub>-(PPO)<sub>69</sub>-(PEO)<sub>99</sub>, MW: 12600 Da] was obtained from BASF corporation. Acryloyl Chloride, anhydrous N-Methyl-2-pyrrolidinone (NMP), sodium acrylate (97%) and poly ethylene glycol (PEG, Molecular wt: 1500 Da) were purchased from Sigma Aldrich. The solvents were of analytical grade. All reagents were used as received without further purification. Irgacure 2959 (4-(2-hydroxyethoxy) phenyl-(2-hydroxy-2-propyl) ketone) was obtained from Ciba for use as a photo-initiator. Fisherbrand regenerated cellulose tubing (10k Molecular Weight Cut Off, (MWCO), 32 mm flat-width) and dialysis tubing closures were purchased from Spectrum Laboratories. 3T3-L1 preadipocyte cell line used for cell studies was purchased from American Type Culture Collection (ATCC). Reagents for cell studies were obtained from multiple suppliers. Dulbecco's modified eagle's medium was purchased from Sigma Aldrich and Dulbecco's phosphate buffered saline was obtained from Gibco. Live/Dead cytotoxicity assay kit and MTS reagent for cell based assays were obtained from Invitrogen and Promega, respectively. Tissue culture dishes and cell culture multi-well plates were obtained from Fisher Scientific.

## 3.2 Chemical Modification of Pluronic F-127

Hydroxyl groups of F-127 were acrylated by reacting F-127 (10 g, 0.8mmol) with ten-fold molar excess of acryloyl chloride. F-127 was completely dissolved in 200 mL NMP with stirring in a 500 mL round bottom flask. The resultant solution was purged with nitrogen. Acryloyl chloride (8 mmol) was dissolved in 50 mL NMP and was added drop-wise into the Pluronics mixture over a duration of 3 hours with continuous stirring at 1200 rpm. The mixture was then allowed to react for 48 hours to complete the reaction. The resulting mixture was purified by dialysis (regenerated cellulose tubing, 10k MWCO), followed by freeze drying (Millrock bench-top freeze dryer) to obtain the final product. Di-acrylated F-127 was sealed and stored in glass vials in the refrigerator. The reaction for the formation di-acrylated F-127 (DA-F127) is shown below.

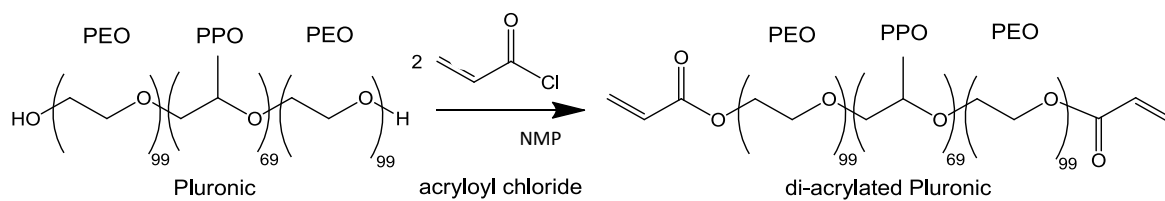


Figure 3.1: Esterification reaction of Pluronic F127 with acryloyl chloride

## 3.3 Gel Composition and Preparation

Gels were prepared by dissolving the required quantities of polymers and photo-initiator in deionized water to make 30% (w/v) solutions.



In the first part of the study, gels were made of only one polymer, DA-F127. Later, it was discovered that the polymer networks formed from DA-F127 would have a very small pore size, in the order of nanometers (nm). Gels containing a mixture of polymers, DA-F127 and poly ethylene glycol (PEG – 1500 Da), in 2:1 ratio were then used to make the hydrogels. DA-F127 would participate in cross-linking due to the presence of terminal acryl groups. PEG would not participate in the cross-linking reaction and could be leached out from the network after cross-linking, thereby making the network relatively porous.

Appropriate quantities of the polymers and 0.05% w/w photo-initiator, Irgacure 2959 were weighed and dissolved in deionized water to form the gel. The sol-state solution was placed at 4°C overnight for homogenous mixing. All hydrogels used in this study were prepared in the same manner unless otherwise specified.

### **3.4 Gamma Irradiation**

5 ml gel samples of DA-F127 and Pluronic F-127 in plastic vials were exposed to varying gamma radiation dosages from 2 Gy (1 Gray = 100 rad/s) to 40 Gy at intervals of 2 Gy. The instrument used for this experiment was 2100 IX, Varian Medical Systems. The facility at the Stony Brook University Hospital was used for this study. The irradiated samples were freeze dried to obtain the dried polymer for further analysis.

### 3.5 UV Radiation Induced Photo Cross-linking

The hydrogels with 0.05% w/w photo-initiator were cross-linked with X11500 Spectrolinker from Spectronics Corporation ( $\lambda$ : 254 nm; Intensity: 5500  $\mu\text{W}/\text{cm}^2$ ). Hydrogel samples were exposed to UV radiation for a period of 30 minutes to obtain cross-linked gels. Cross-linking was confirmed from rheology measurements before and after UV irradiation.

1 mL hydrogel samples were placed in shell vials (7 dr, O.D.xH: 29 x 65 mm; fisherbrand) and irradiated without closures. All the photo-crosslinking experiments were performed in the same manner, unless otherwise specified.

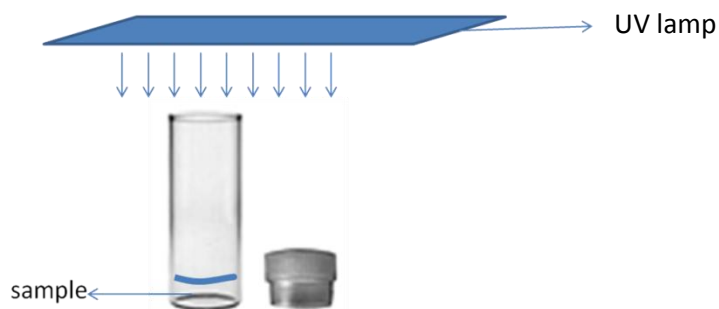


Figure 3.2: UV irradiation of Diacrylated-F127

### 3.6 Swelling Studies

30% w/w (2:1, DA-F127: PEG 1.5 kDa) gels, exposed to UV radiation for 30 minutes were used to study the swelling behavior. Deionized water, which was stirred continuously at 150 rpm, was the medium used for swelling the samples. The gels were placed in centrifuge tubes having 3 mm diameter perforations to ensure continuous flow of swelling medium around

the gels. All the centrifuge tubes were placed in a large vessel containing the medium at  $37 \pm 0.5$  °C. The medium was changed every day.

In the swelling study, weights and dimensions of the gels were measured at definite time points. Before measuring, the gel was removed from the swelling medium and was dabbed with Kimwipe® on the surface to remove any excess water.

### **3.7 Storage Modulus**

The mechanical properties of the hydrogels were evaluated by measuring the storage modulus ( $G'$ ), using the Anton Paar Physcia MCR 301 rheometer. All measurements were made at  $37 \pm 0.5$  °C to mimic body conditions. A cone - plate geometry was used, with angular frequencies ranging from 0.1 Hz to 100 Hz, and a constant strain of 2%.

Cross-linked 30% w/w (2:1 ratio of DAF127: PEG, 1.5 kDa) gel samples were immersed in deionized water for swelling. The storage modulus of the swollen gels was monitored for a period of 10 days.

### **3.8 Cell Studies**

All the cell studies were performed using 3T3-L1 cell line procured from the American Type Culture Collection (ATCC). 3T3-L1 cell line consists of mouse embryonic fibroblasts. These cells are preadipocytes and have a doubling time of approximately 14 hours. The base medium for this cell line is Dulbecco's Modified Eagle's Medium (DMEM). The base medium supplemented with bovine calf serum and penicillin was the recommended growth medium for

these cells and the same was used. The culture was not allowed to reach confluency as per the protocol. The subcultures were prepared by the procedure described below:

- i. The frozen vial obtained from ATCC, containing the cells was warmed to obtain a cell suspension
- ii. The solution was transferred to a 15 mL centrifuge tube
- iii. 1 mL of growth medium was added to the centrifuge tube and the solution was centrifuged at 1000 rpm for 5 minutes. After centrifugation, cell pellet was formed at the bottom of the centrifuge tube
- iv. The medium was aspirated and the cells were redispersed in approximately 5 mL growth medium
- v. The solution was transferred into a tissue culture dish and an additional 5 mL growth medium was added
- vi. The cells were incubated at 37 °C
- vii. The growth medium in the tissue culture dish was replaced every 2 days. The cells were allowed to reach approximately 60% confluency
- viii. Cells were then counted using the haemocytometer (calculations discussed below)
- ix. Adequate volume of cell suspension was then added to new culture vessels (vials). Additional growth medium was added to the vials to obtain a final volume of 950 µL
- x. 5 % DMSO (50 µL DMSO) was added to each vial (to function as an antifreeze when cells were in frozen state)
- xi. The new vials were kept in the freezer at -72 °C for 24 hours and were stored in liquid nitrogen tanks.<sup>28</sup>

Additional passages were made whenever required by the following procedure:

- i. The medium in the tissue culture dish was aspirated
- ii. The cells were washed twice with 5 mL sterile Dulbecco's Phosphate Buffered Saline
- iii. 5 mL Trypsin/EDTA solution was added to the tissue culture dish and was incubated at 37 °C for 5 minutes
- iv. After 5 minutes, the dish was removed from the incubator and was observed from the bottom to see a cell suspension
- v. 5 mL of growth medium was gently added to the dish such that the cells were unharmed
- vi. The entire solution was taken out and collected in a 15 mL centrifuge tube
- vii. The solution was centrifuged at 1000 rpm for 5 minutes. After centrifugation, cell pellet was formed at the bottom of the centrifuge tube
- viii. The medium was aspirated and the cells were redispersed in approximately 5 mL growth medium
- ix. A small volume of cell suspension was taken in a micro-centrifuge tube and diluted
- x. Cells present in 10  $\mu$ L of the diluted solution were counted using the haemocytometer
- xi. Appropriate volume of cell suspension was then transferred into multiple tissue culture dishes and an additional growth medium was added to each of them to obtain a final volume of 10 mL in each tissue culture dish
- xii. The cells were incubated at 37°C
- xiii. The growth medium was replaced by fresh medium after every 2 days to maintain the cells.

## Cell counting using Haemocytometer:

### A. Preparing haemocytometer

- i. The haemocytometer was cleaned using 70% ethanol
- ii. The shoulders of the haemocytometer were moistened and the coverslip was placed on it using gentle pressure. The phenomenon of Newton's rings can be observed when the coverslip is correctly affixed.

### B. Preparing cell suspension

- i. The cell suspension to be counted was mixed by either gentle agitation of the micro-centrifuge tube containing the cells or by using a pipette if required
- ii. Before the cells had a chance to settle, about 10  $\mu$ l of cell suspension was taken out using a Gilson pipette

### C. Counting

- i. The cell suspension was carefully filled on the haemocytometer by gently resting the end of the Gilson tip at the edge of the chambers. Care was taken not to overfill the chamber. The sample was allowed to be drawn out of the pipette by capillary action
- ii. All the chambers of the grid were filled with cell suspension
- iii. Using the 10X objective of the microscope, grid lines of the haemocytometer were focused. One set of 16 corner square was focused at a time

- iv. Using a hand tally counter, the number of cells in this area of 16 squares was counted. The cells that were within the square and any positioned on the right hand or bottom boundary line were counted.
- v. The haemocytometer was moved to another set of 16 corner squares and counting was repeated until all 4 sets of 16 corner squares are counted.
- vi. The haemocytometer is designed such that the number of cells in one set of 16 corner squares is equivalent to the number of cells  $\times 10^4$  /mL

Therefore, to obtain the count:

The total count from 4 sets of 16 corner = (cells / ml  $\times 10^4$ )  $\times 4$  squares from one haemocytometer grid

- i. The count is divided by 4
- ii. This number is then multiplied by the dilution factor to adjust for the dilution

A schematic of cell counting using a haemocytometer is shown in Figure 3.3<sup>29</sup>

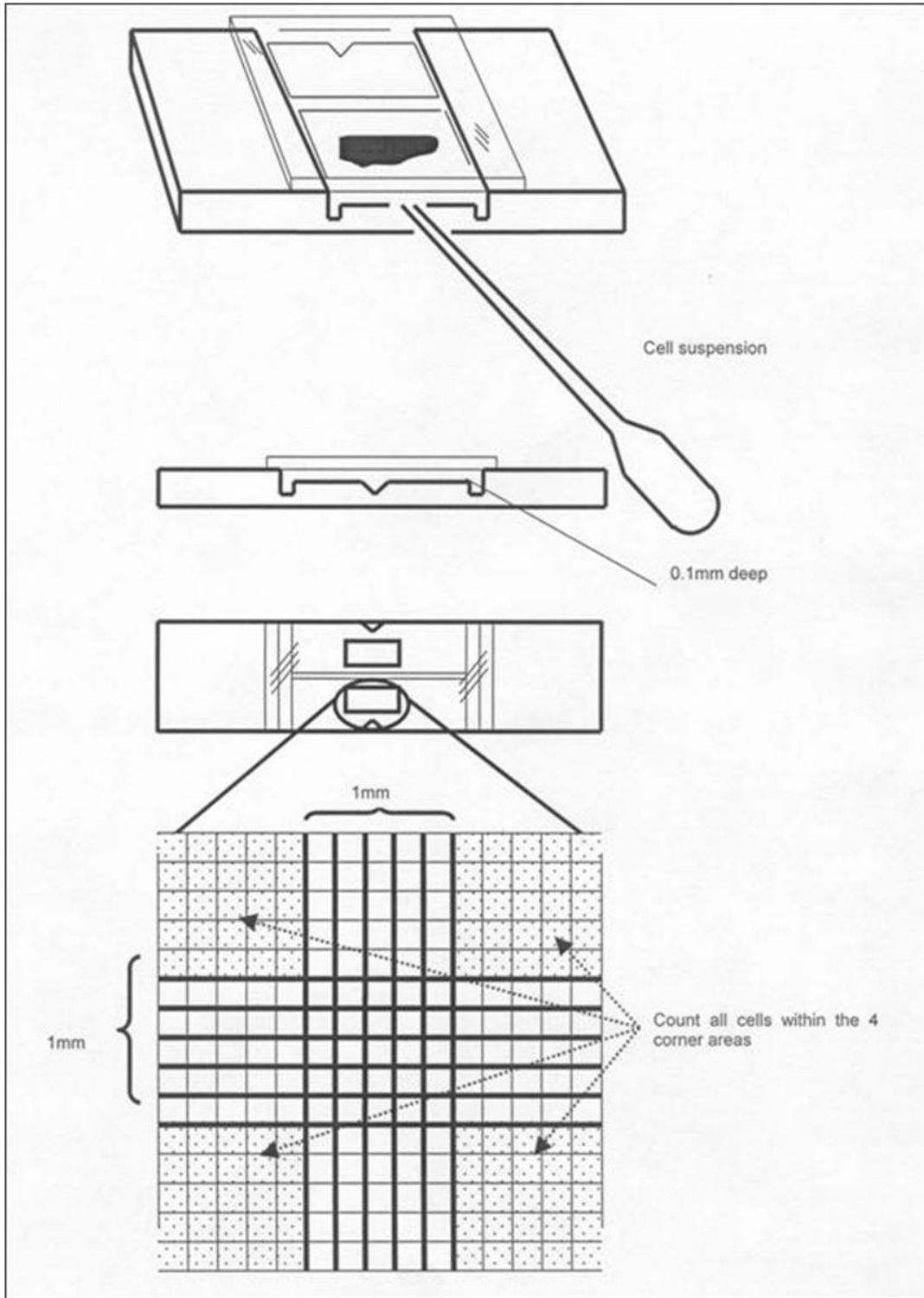


Figure 3.3: Cell counting using Haemocytometer<sup>29</sup>



### 3.8.1 MTS Assay

Two experiments involving MTS assay were performed in our study. The first experiment was performed on the 3T3-L1 cells in the absence of any sample gels to check the efficiency of MTS assay on this preadipocyte cell line. This experiment was performed by placing approximately 36000 cells on a 24 well plate. The cell suspension was placed on each well, followed by the addition of 500  $\mu$ L of growth medium in each well. The control group consisted of wells containing growth medium.

The second experiment was performed with 30% w/w gels of diacrylated F-127. The gel samples were sterilized by exposing them to UV radiation for 5 minutes under the tissue culture hood. 0.5 mL gel samples were placed in each well. Cell suspension consisting of approximately 45000 cells was added onto each of these samples. 500  $\mu$ L of growth medium was added to each well plate. The control samples for this study consisted of wells containing cell suspension and growth medium, with no gel sample.

In each of the above experiments, at the required time points, the growth medium was aspirated from the wells of the cell culture plate. This was followed by addition of 50  $\mu$ L MTS reagent onto the cells along with 200  $\mu$ L growth medium. The cells were then incubated for 40 minutes at 37 °C. After the incubation period, the solution was transferred to a new well plate and the absorbance at 490 nm was measured by the KC Junior spectrophotometer (Bio-Tek Instruments Inc).

### 3.8.2 Live/Dead Assay

Visual images of cells in DA-F127 gels and control samples were obtained from the live-dead assay. The test sample consisted of 30% w/w gel of DA-F127. The control sample consisted of a similar gel made from Pluronic F-127. Approximately 0.5 mL gel samples were placed in a 12 well plate. Cells dispersed in growth medium were placed on each of these gels. Each well was then covered by 1 mL growth medium (DMEM). At definite time intervals, cells were taken out, stained and imaged using Zeiss microscope in the Biomedical Engineering department of Stony Brook University. Time points used for this study were 30 mins, 2 hr, 6 hr, 12 hr and 24 hr.

The assay procedure involves three steps: The first step is cell preparation. This is followed by determination of optimal dye concentration. The last step is performing the viability assay which involves incubating the cells followed by imaging.

The cells were first washed twice with sterile phosphate buffered saline (PBS) to remove or dilute serum esterase activity present in the serum-supplemented growth medium. An aliquot of cell suspension was transferred onto a new tissue culture well plate.

To prepare the required dye concentrations, the live/dead reagent stock solutions were removed from the freezer and were allowed to warm to room temperature. 6.5  $\mu$ L of the supplied EthD-1 stock solution was added to 1.3 mL of sterile PBS. The solution mixture was vortexed to ensure thorough mixing. The reagents were combined by transferring 3.25  $\mu$ L of the original calcein AM stock solution to EthD-1 solution. The solution was thoroughly mixed by vortexing. This solution was added directly to the cells.

100  $\mu$ L of the combined live/dead assay reagent was added to the well containing the cell suspension such that all the cells were covered with reagent. The cells were incubated for 30

minutes at room temperature. Incubations were done in a covered dish to prevent contamination or drying of the samples. The cells were viewed and imaged under the Zeiss microscope. The fluorescence from these dyes was viewed simultaneously with a fluorescein longpass filter.

### 3.8.3 Photo-initiator cytotoxicity

Irgacure 2959 (4-(2-hydroxyethoxy)phenyl-(2-hydroxy-2-propyl) ketone) was used as the photo-initiator for cross-linking of the DA-F127 hydrogels.

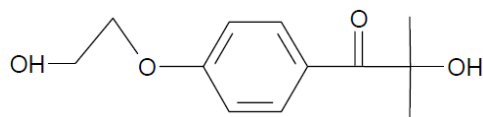


Figure 3.4: Irgacure 2959

Cytotoxicity of Irgacure 2959 was investigated on 3T3-L1 cells. 600,000 3T3-L1 cells were seeded in each well of a 24-well cell culture plate. Aqueous solutions of 0.025%, 0.05%, and 0.075% w/v Irgacure 2959 were placed on the cells. Cells exposed to deionized water served as the control group. After two days, cells were stained with Trypan blue and the viable cells were counted using the haemocytometer.

To count the number of viable cells, an aliquot of cell suspension was centrifuged for 5 minutes at 1000 rpm. The cell pellet was resuspended in DMEM. 1 part of 0.4% trypan blue was mixed with 1 part cell suspension and the mixture was incubated for approximately 2 minutes at room temperature. The suspension was then mounted onto a haemocytometer and the cells were counted. Cells were counted within 3 to 5 min of mixing with trypan blue, since longer

incubation periods lead to cell death and reduce the viability counts. The unstained cells (viable) and stained (non-viable) cells were counted separately.

### **3.8.4 Cell studies with cross-linked gel**

30% w/w gels consisting of 2:1 ratio of DA-F127: PEG (1.5 kDa) was used for this study. The gels were prepared by dissolving the appropriate quantities of polymers and 0.05% w/w photo-initiator in de-ionized water. A homogenous mixture was obtained by refrigerating the mixture overnight at 4 °C. The gels were transferred into a 24 cell culture multi-well plate with 0.5 mL of gel in each well. The gels were cross-linked by exposing them to UV radiation for 30 minutes. The cross-linked gels were allowed to remain in the multi-well plate for approximately 18 hours. They were then removed from the plates to obtain cross-linked polymer disks. Each of these disks was immersed in DMEM for approximately 24 hours.

The cross-linked polymer disks equilibrated with DMEM were used as the test samples for cell study. Each polymer disk was placed in a 35 mm tissue culture dish. Cell suspension consisting of approximately 50,000 cells was placed on each of these gel samples and the same volume was also placed adjacent to the sample gel. The samples were then incubated for approximately 45 minutes. After 45 minutes, 2 mL growth medium was added to the tissue culture dishes. The control samples for this study consisted of cell suspension and growth medium (with no sample gel). The cells were observed under the microscope and imaged by phase contrast microscopy on day 3.

### **3.9 Sodium Acrylate Cross-linking**

This study was done to check the ability of sodium acrylate to crosslink with UV radiation in the presence of 20% Pluronic copolymer. 30% w/w hydrogels of F-127 and sodium acrylate in 2:1 ratio were prepared by dissolving appropriate quantities in deionized water. 0.05% w/w photo-initiator was added to enable UV initiated photo-cross-linking. 2 mL hydrogel samples were placed in shell vials (7dr, O.D.xH: 29 x 65mm; fisherbrand) and irradiated in the absence of a closure.

Polymerization of sodium acrylate was confirmed by performing viscosity measurements on the gels at  $30 \pm 0.5$  °C before and after UV irradiation. The measurements were made by the Anton Paar Physicia MCR-301 rheometer.

### **3.10 Scanning Electron Microscopy**

SEM studies were performed on the cross-linked gels to check the presence of pores. The cross-linked polymer networks were swollen for 7 days in deionized water and the swollen gels were used as samples for the study. The cross-sectioned samples were prepared by fracturing the water-wetted membrane in a liquid nitrogen bath. Scanning electron microscope (LEO 1550) equipped with a Schottky field emission gun (10 kV) and a Robinson backscatter detector was used for taking the SEM micrographs.

### **3.11 Small Angle X-ray Scattering**

Small-angle X-ray scattering (SAXS) measurements were carried out at the X27C beamline in the National Synchrotron Light Source (NSLS), Brookhaven National Laboratory (BNL). The X-ray wavelength was set at 1.371 Å. Two-dimensional (2D) SAXS patterns were acquired using a MAR-CCD detector. The typical image acquisition time for each scan was 120 seconds. Silver behenate was used as a standard to calibrate the scattering angle. The sample-to-detector distance was 1762 mm. X-ray measurements for all samples were taken under the same conditions at room temperature. All scattering or diffraction signals were corrected for beam fluctuations, sample absorption and background scattering. Data analysis was performed using the software Polar (Stony Brook Technology and Applied Research, Stony Brook, New York)

Three types of gel samples were used for this study. The first sample consisted of 30% w/w gels of 2:1 ratio of DA-F127: PEG (1.5 kDa). The second and third samples consisted of 20% w/w and 30% w/w gels of DA-F127 respectively. All the gels were cross-linked by UV radiation for a period of 30 minutes.

# Chapter 4

## Results and Discussion

This chapter discusses the rationale of all the experiments performed in detail, along with the expected results and gives the implication of the results obtained.

### 4.1 Chemical Modification of Pluronics

The extent of acrylation from the esterification reaction discussed in the experimental section was determined by  $^1\text{H-NMR}$  (300 MHz). The chemical shift ( $\delta$ ) was measured in ppm using deuterated DMSO as the internal reference. The average degree of acrylation for all the reaction batches was found to be approximately 85-95%. This is estimated by comparing the acryl protons of diacrylated F-127 ( $=\text{CH}_2$ , 5.8 – 6.4 ppm) and three protons of the methyl group of the propylene oxide unit ( $-\text{CH}_3$ , 1.1 ppm).

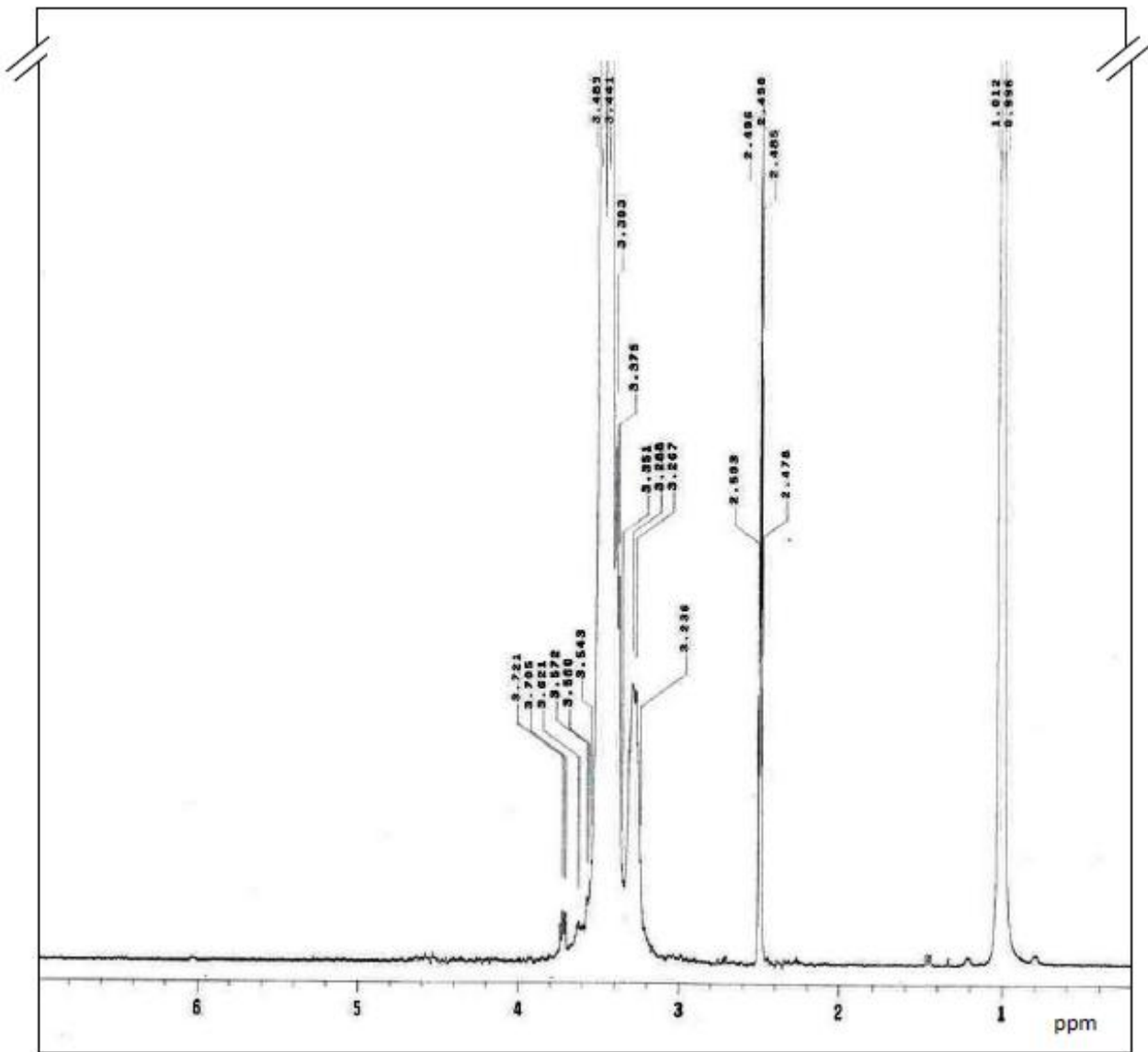


Figure 4.1:  $^1\text{H-NMR}$  Spectrum of Pluronic F-127



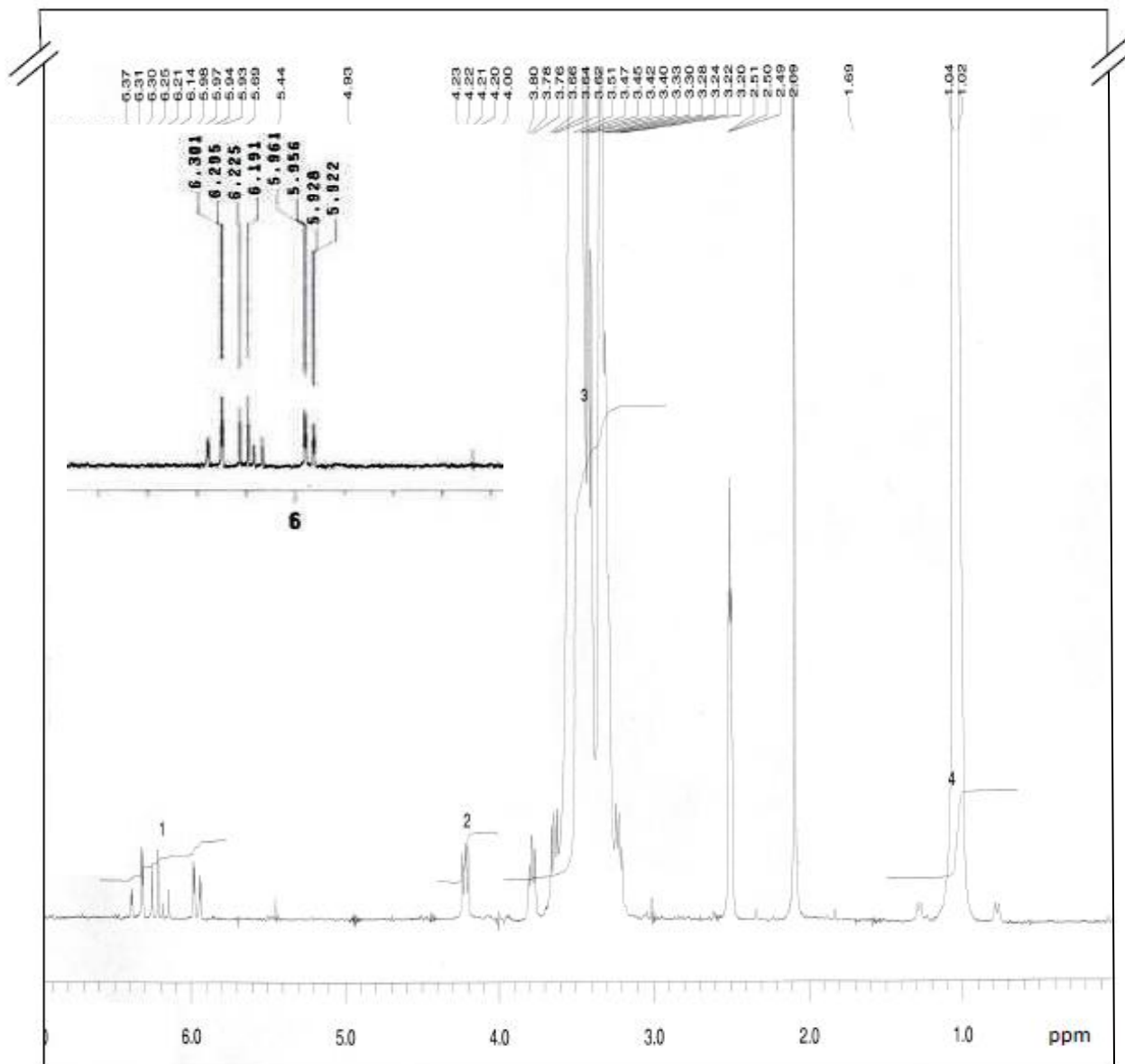


Figure 4.2:  $^1\text{H-NMR}$  Spectrum of Diacrylated F-127 (Inset: 5-7 ppm portion of spectrum)

## 4.2 Gamma Radiation

Cross-linking with gamma irradiation is a widely used technique. An advantage of using gamma radiation for cross-linking is that the radiation is very penetrating and the technology is

very simple, thus resulting in a low downtime for gamma radiation source. Post lumpectomy breast cancer patients usually undergo gamma radiation therapy after tumor removal. In this therapy, patients are exposed to a total gamma radiation dosage of 40 Gy in multiple sittings with a dosage of 2 Gy in each sitting. Hence, gamma irradiation experiments were performed with varying dosages from 2 Gy to 40 Gy at intervals of 2 Gy to check the possibility of any cross-linking.<sup>30,31</sup>

The irradiated samples were dried by freeze drying. The samples were analyzed by <sup>1</sup>H-NMR spectroscopy to check for cross-linking by comparing the signal of the acryl protons with the original DA-F127. The resulting spectrum was similar to that obtained from DA-F127, thus indicating absence of any significant cross-linking.

A gamma radiation dosage as high as 40 Gy (maximum dosage received by breast cancer patient) did not have any significant effect on the DA-F127 and F-127 hydrogels. This implies that these hydrogels are resistant to the gamma radiation therapy that most of the post-lumpectomy patients undergo.

### **4.3 UV Radiation Induced Photo Cross-linking**

Initially, the hydrogel samples were irradiated with long wavelength UV radiation in the absence of any photo-initiators. In earlier studies, it was hypothesized that by conjugating acrylate groups to the terminal ends of a Pluronics copolymer, a photo-crosslinkable hydrogel could be obtained even in the absence of any additional polymerization aiding agents. Photopolymerization was expected to occur due to the presence of enriched acrylate groups present in the interstitial space between the self-assembled Pluronics micelles.<sup>25</sup> The polymers were thus

exposed to UVA without incorporating any photo-initiator. The irradiated samples were later freeze dried to obtain the dried polymer which was analyzed by  $^1\text{H-NMR}$  spectroscopy. The  $^1\text{H-NMR}$  spectra was similar to that of the original DA-F127 spectrum and thus did not reveal any significant cross-linking of the polymer.

In the photo-polymerization reaction, reactive free radicals are produced from the photo-initiator by photo-cleavage. These initiators attack the vinyl groups at the ends of the Pluronics, converting them into reactive radicals resulting in the polymerization of DA-F127.<sup>32,33</sup> Thus, vinyl groups present on the periphery of Pluronics micelles can be polymerized to covalently crosslink the closely packed micelles in the DA-F127 gel. This produces the cross-linked DAF127 hydrogel networks.

Figure 4.3 provides a schematic representation of the gelation of DA-F127 with an increase in temperature, followed by photo-polymerization.

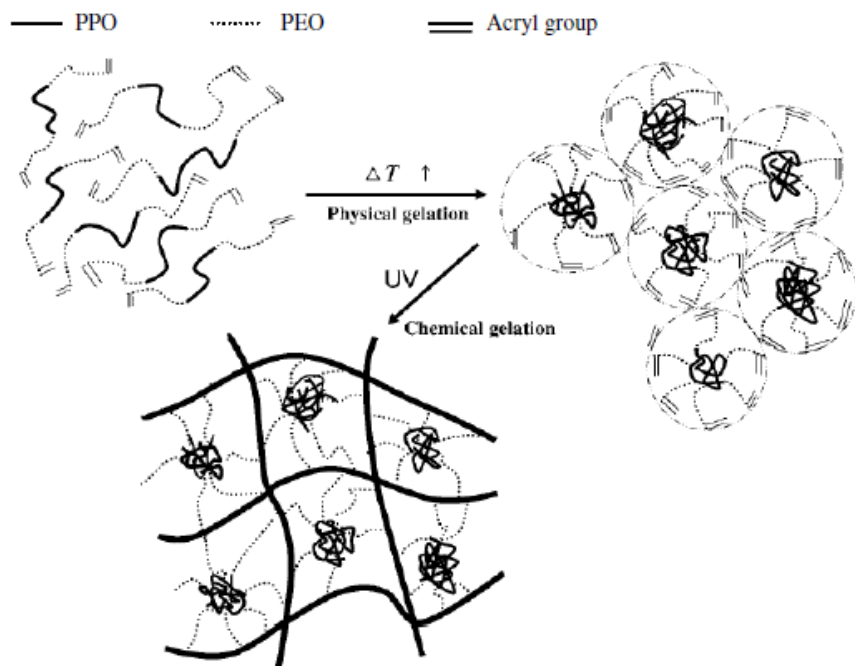


Figure 4.3: UV radiation induced photo-polymerization reaction<sup>25</sup>

Initially the DA-F127 polymers would exist in the form of micelles at room temperatures and as individual unimers at low temperatures. When radicals are generated by UV irradiation, they produce reactive polymeric micelles at room temperature. The generated reactive micelles increase in number as small-sized clusters connected by a few micelles, instead of forming large, three dimensional networked structures immediately. When adequate numbers of such small clusters are generated, they crosslink with each other, resulting in macroscopic gelation or, in other words, polymer network formation, that causes rapid increase in the viscosity and the modulus of the hydrogel.<sup>33</sup> It should be noted that we can take advantage of the temperature dependence in the initial micelle formation to partially control the polymer network formation. This feature has not yet been investigated.

Latter experiments were performed by irradiating 30% (w/w) gel samples in the presence of 0.05% (w/w) photo-initiator, Irgacure 2959. Upon incorporation of the photo-initiator, it was visually observed that the viscosity of the irradiated samples increased significantly and the cross-linked sample was no longer thermo-reversible. The original hydrogel transformed into an elastic, rubber-like disk after UV irradiation as shown in Figure 4.4. The samples were freeze dried to obtain the dried polymer for further analysis to confirm cross-linking. However, the freeze-dried polymer could not be analyzed by <sup>1</sup>H-NMR due to its poor solubility in the solvent, deuterated dimethyl sulfoxide (DMSO-d<sub>6</sub>), caused by cross-linking.

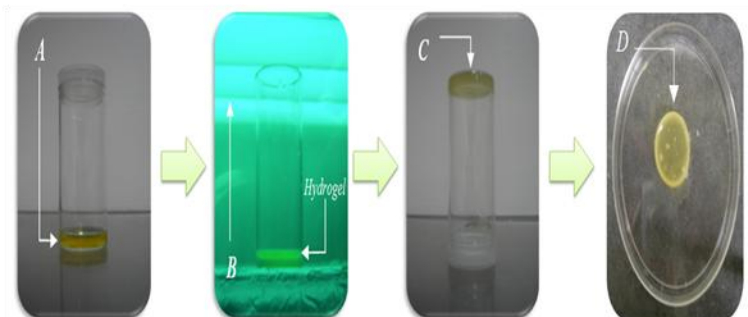


Figure 4.4: Formation of cross-linked DA-F127 polymer network (A) DA-F127 gel, (B) UV irradiation, (C) Cross-linked hydrogel, (D) Cross-linked polymer disk

## 4.4 Swelling Studies

During the swelling study, the weights and the dimensions of the gels were obtained at definite time points over a period of two weeks.

Swelling ratio was computed by the following equation:

$$\text{Swelling ratio} = (W_s - W_d) / W_d$$

Where  $W_s$  is the weight of the swollen hydrogel and  $W_d$  is the weight of the dry hydrogel.<sup>34</sup>

The results can be seen in Figure 4.5. As can be seen from the swelling plots, the gels were swollen to a large extent in the first 5 days. The rate of swelling was slow after 5 days and the sample appears to have reached equilibrium in two weeks. The volume of the gels was also measured, since the change in volume should be crucial during implantation. The gel should not swell to a large extent after implantation, because increase in volume after implantation might result in undesirable immune responses.

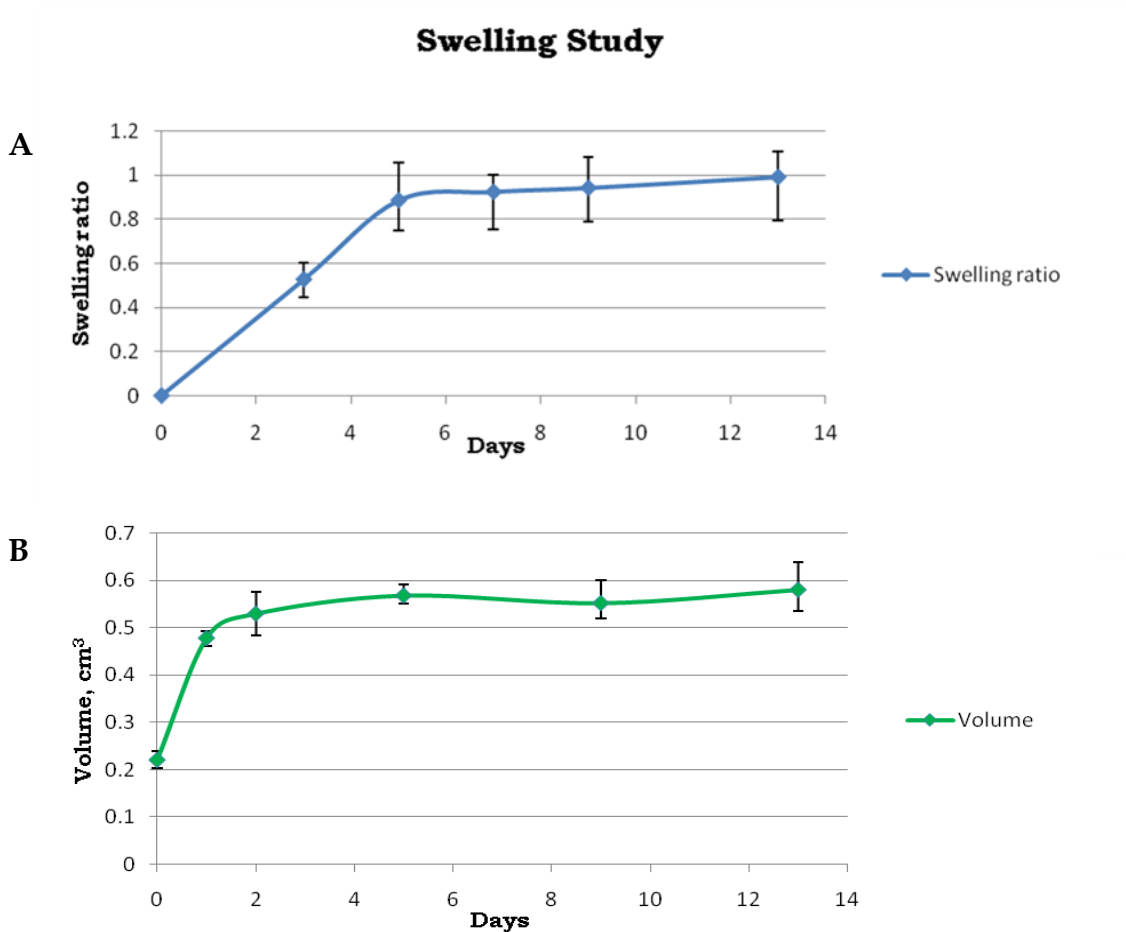


Figure 4.5: Swelling study, (A) Swelling ratio, (B) Change in gel volume

## 4.5 Storage Modulus

The storage modulus provides information about the elastic portion of the gel. The storage modulus values of the human adipose tissue are in the range of 11 – 40 kPa.<sup>35,36</sup> It was observed that the values of the storage modulus of the cross-linked hydrogels were comparable to those of the human adipose tissue. The storage modulus values dropped significantly during the swelling process. However, the storage modulus of the equilibrated samples was in the

required range. It should be noted that the hydrogels can be made stronger if required, by increasing the UV radiation time.

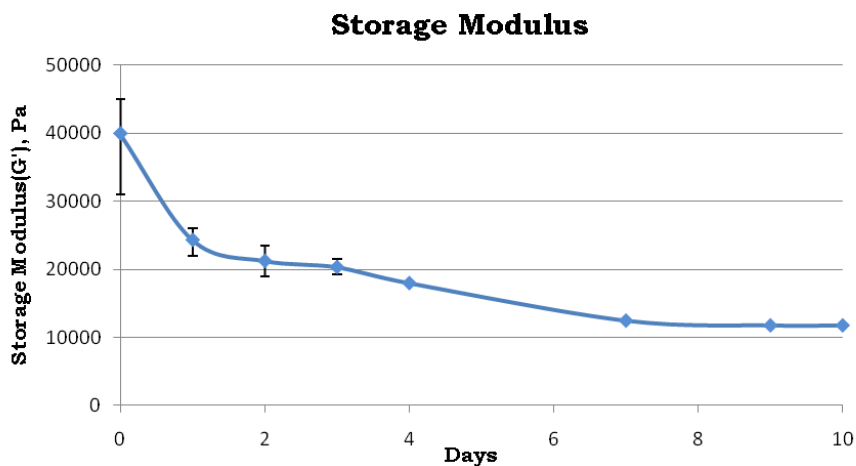


Figure 4.6: Change in storage modulus of cross-linked DA-F127 during swelling

## 4.6 Cell Studies

Mature adipocytes are the predominant cell type in the adipose tissue. However, use of preadipocytes is more favorable for studying scaffold designing. Results from previous studies have indicated that mature adipocytes do not yield good results. Mature adipocytes are too fragile, and do not proliferate since they are fully differentiated. Preadipocytes, on the other hand, are not differentiated and can thus be expanded *in vitro*.<sup>37</sup> Also, preadipocytes can tolerate extreme environments and are thus favorable for our study.

Multiple cell studies were performed to analyze toxicity of various components of the polymer network. The initial studies were performed to measure efficiency of specific techniques

with the chosen preadipocyte cell line. Non cross-linked DA-F127 gels were used in the initial studies, to evaluate toxicity. The final study was performed with the cross-linked polymer network.

#### **4.6.1 MTS Assay**

The CellTiter Aqueous Non-Radioactive Cell Proliferation Assay (MTS Assay) was utilized to measure cell viability and cell growth. MTS reagent is a yellow solution containing tetrazolium compound [3-(4,5-dimethylthiazol-2-yl)-5-(3-carboxymethoxy phenyl)-2-(4-sulfophenyl)-2H-tetrazolium, inner salt] (MTS) and phenazine methosulfate (PMS), which is an electron coupling reagent. The tetrazolium salt has an absorbance maximum at 490-500 nm. Active enzymes present in viable cells bio-reduce the MTS to formazan, which has a purple-black color. This conversion is most likely accomplished by NADPH (nicotinamide adenine dinucleotide phosphate-oxidase) or NADH (reduced nicotinamide adenine dinucleotide) produced by dehydrogenase enzymes in metabolically active cells.<sup>38</sup> The reduction occurs only when the enzymes in the cells are active, and thus the conversion is often used as a measure of viable cells. This assay thus measures the activity of cells which in turn corresponds to the number of healthy cells, thus indicating cell growth.<sup>39</sup> When the amount of formazan produced by cells treated with an agent is compared with the amount of formazan produced by untreated control cells, the effectiveness of the agent in causing death, or changing the metabolism of cells, can be deduced.



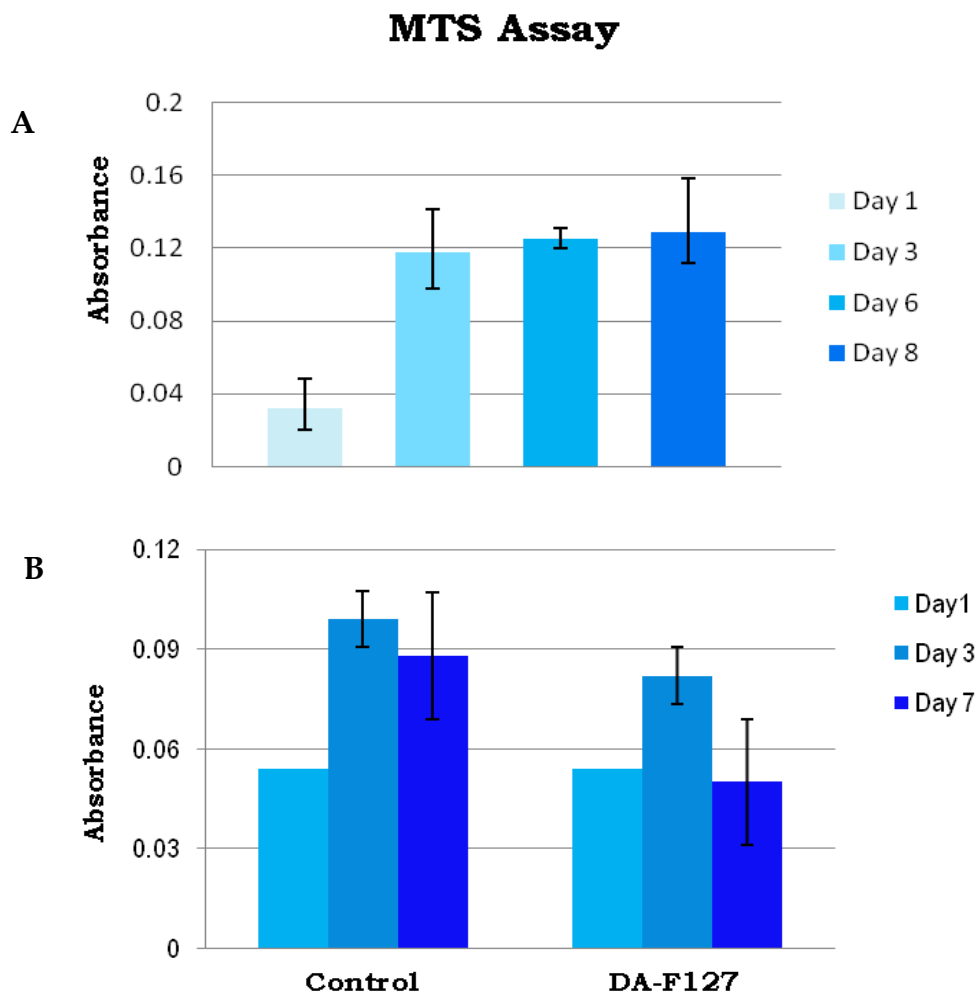


Figure 4.7: MTS Assay of A: Cells, B: DA-F127 gel

Figure 4.7 shows the graphs of the MTS assay. From the first plot, it is seen that the absorbance values increase from Day 1 to Day 8. There is a sudden increase in absorbance from Day 1 to Day 3 after which the rate slows down. This can be explained by the phenomena of ‘contact inhibition’. It is a process where the cell growth stops or the cells stop dividing as a result of two or more cells coming into contact with each other. Thus, the rate of increase in absorbance was seen to lower after Day 3.

In the second plot, absorbance of both the control and the gel sample increased from Day 0 to Day 3 but dropped on Day 7. During experimentation, it was observed that the DA-F127 hydrogel was completely degraded by Day 7. Thus, the cells did not have a good substrate for cell attachment and growth as a result of the presence of large number of polymer particles and also due to contact inhibition. Since the absorbance in the control wells also dropped from Day 3 to Day 7, it is certain that contact inhibition occurred as a result of which, cells stopped growing. This thus resulted in the death of some cells accompanied by the decrease in cell activity. The DAF-127 hydrogels were proved to be not cytotoxic as the cells multiplied until Day 3 and were also viable on day 7. DAF-127 hydrogels thus did not inhibit cell growth, as confirmed by the increase in activity between day 1 and day 3. The lack of toxicity of the gel was further confirmed by other experiments.

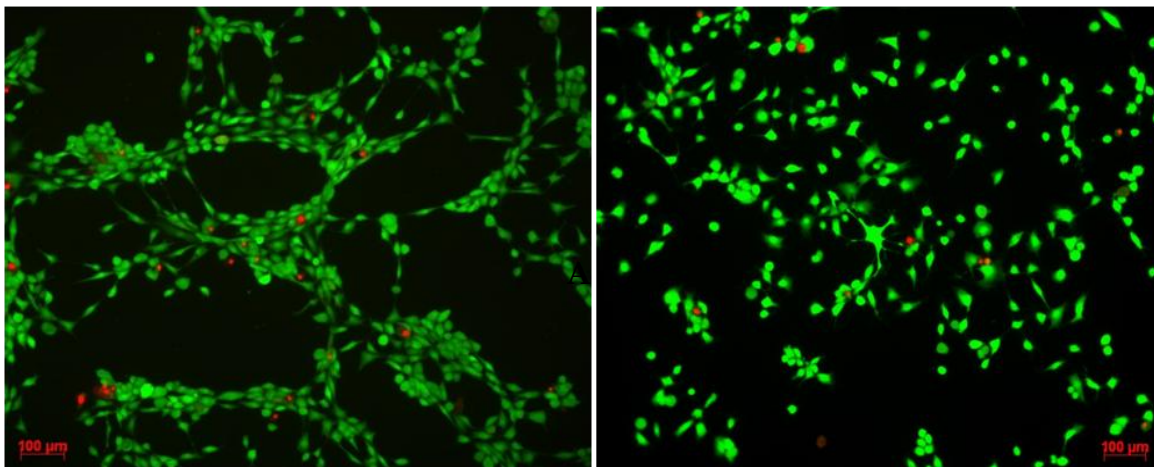
#### **4.6.2 Live – Dead Assay**

The Live/Dead viability assay is a two-color fluorescence cell viability assay which is based on simultaneous determination of live and dead cells with two probes which measure intracellular esterase activity and plasma membrane integrity, which are known parameters of cell viability. The assay consists of two reagents, calcein AM and ethidium homodimer-1 (EthD-1). The live/dead assay provides a more sensitive indicator of cytotoxicity and cell damage.

The live cells are detected by the presence of ubiquitous intracellular esterase activity. Non fluorescent cell permeant calcein AM is converted to intensely fluorescent calcein by the esterase enzyme. The polyanionic dye calcein is well retained in live cells and produces an intense green fluorescence in live cells (excitation/emission ~495 nm/~515 nm). EthD-1 enters

the dead cells which have damaged membranes and undergoes a 40-fold enhancement of fluorescence upon binding to the nucleic acids in the cells, thus producing a bright red fluorescence in dead cells (excitation/emission ~495 nm/~635 nm). EthD-1 is excluded by the intact plasma membrane of live cells. Cell viability is thus determined by these physical and biochemical properties of the cells.<sup>40</sup>

Since the dyes are virtually non-fluorescent before interacting with cells, this assay technique has very low background fluorescence levels.



**A**

**B**

Figure 4.8: Live Dead assay images, (A) Control, (B) 30% w/w DA-F127 gel; green dots: live cells, red dots: dead cells

Figure 4.8 shows the presence of very few dead cells (represented by red dots) in both the control and the test samples. This assay thus further confirmed the results obtained from MTS assay, thus proving that DA-F127 gel is not cytotoxic.

### 4.6.3 Photo-initiator cytotoxicity

Cytotoxicity of the photo-initiator plays an important role since the cells have to be tolerant to low concentrations of the photo-initiator which may possibly remain after the cross-linking reaction.

Irgacure 2959 is one of the most popular photo-initiators for tissue engineering applications due to its high solubility in water and its minimal toxicity compared to other species.<sup>41</sup> Its cytotoxicity was evaluated by exposing the cells to multiple concentrations of aqueous solutions of Irgacure 2959. Cytotoxicity of Irgacure 2959 was determined by staining the cells with Trypan Blue and counting the number of viable cells. Trypan blue staining technique is based on the principle that live cells possessing intact cell membranes exclude dyes such as trypan blue.<sup>42</sup> The viable cells have a clear cytoplasm while the dead cells have blue colored cytoplasm when observed under the microscope.

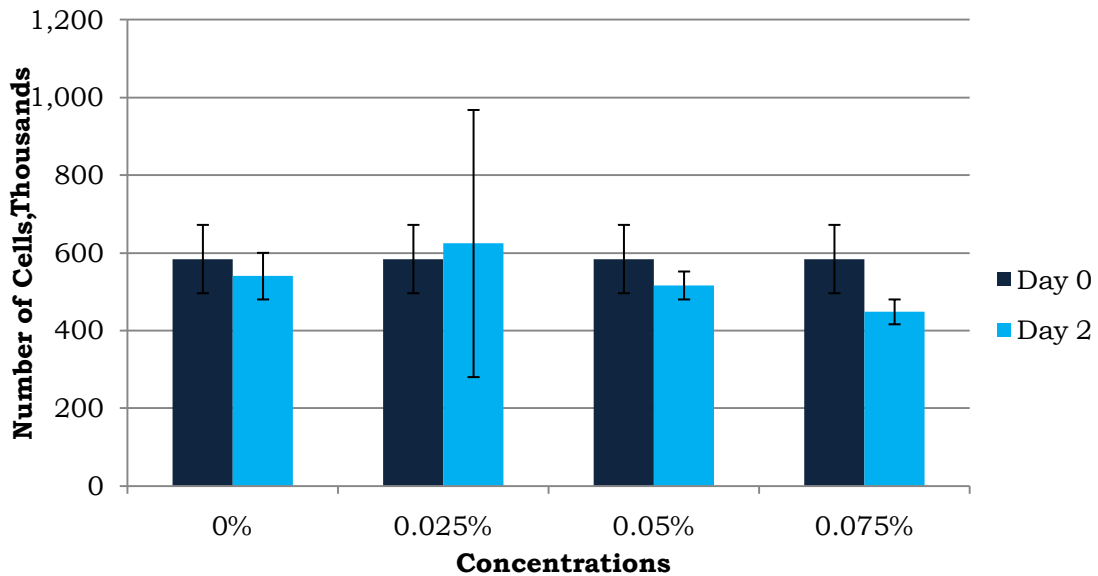


Figure 4.9: Photo-initiator cytotoxicity from Trypan Blue staining

In Figure 4.9, it can be seen that the number of 3T3-L1 preadipocyte cells decreased by a small amount by day 2 in all the groups, including the control group. This can be due to seeding of excess cells in each well of the 24-well culture plate. With 600,000 cells in each well, the cells reached contact inhibition by day 2, ensuing in cell death. Upon observation under the microscope, the cells looked healthy and exhibited spindle-like morphologies. Thus the photo-initiator was not cytotoxic to the cells at the three concentrations tested. Consequently, Irgacure 2959 was chosen as the suitable photo-initiator for our application.

#### **4.6.4 Cell studies with cross-linked gel**

Cross-linked gel samples saturated with DMEM were studied for toxicity. On day 3, the tissue culture dishes were removed from the incubator. The growth medium surrounding the gel was removed and the tissue culture dish was rinsed twice with fresh growth medium. The polymer networks were imaged with Zeiss microscope to check for the presence of cells. The images were obtained by Phase contrast microscopy (Figure 4.10).

In (A) it can be seen that no cells were present on the surface of the gel (gel: bright pink color). However, a large number of healthy, live cells were present around the gel as seen in (B). This implied that the surface of the gel did not favor cell adhesion. The gel, thus did not act as a good substrate for cell adhesion. The presence of healthy cells adjacent to the gel indicated that the cross-linked polymer network was not toxic for the cells. The presence of the polymer did not hinder cell division and cell proliferation, as can be seen from the images of the cells in Figure 4.10 (B) and (C).

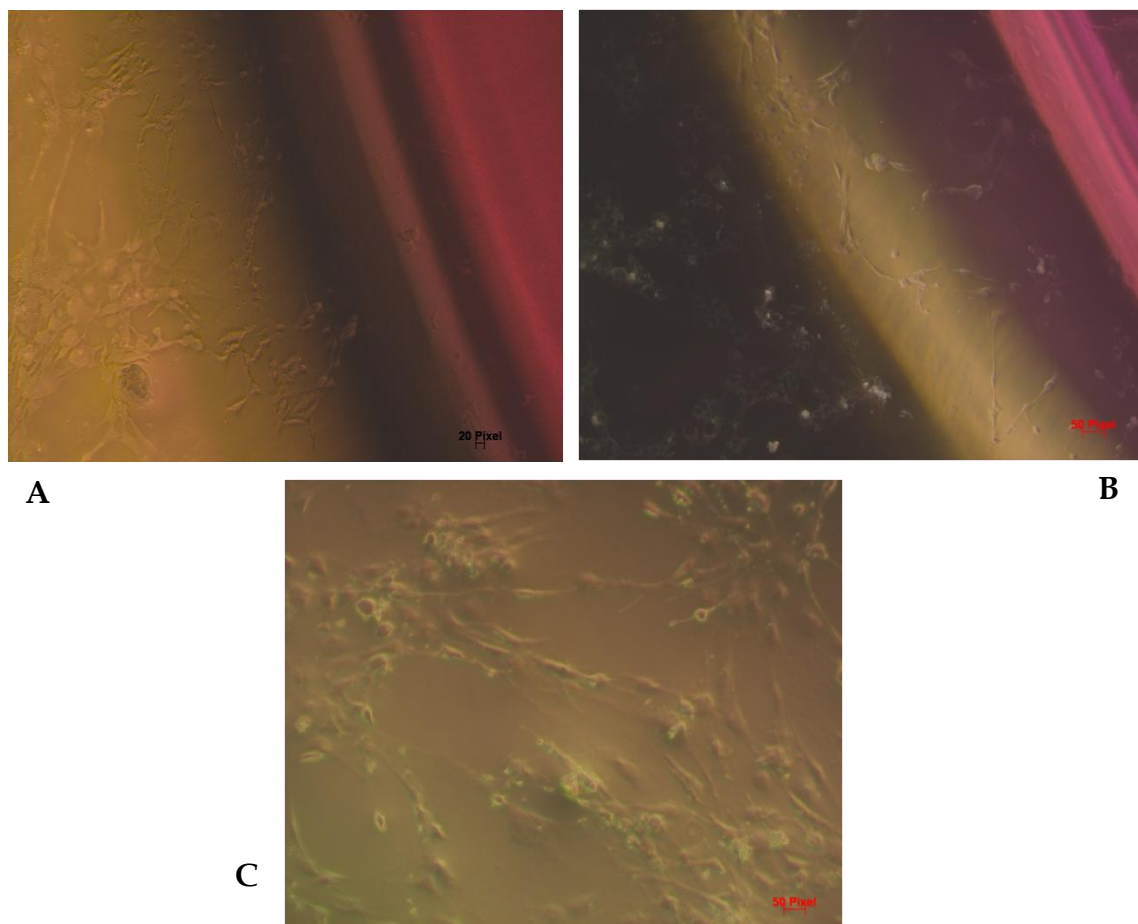


Figure 4.10: (A),(B) Gel sample with cells, (C) Cells adjacent to gel (gel is pink)

## 4.7 Sodium Acrylate Cross-linking

The cross-linked Pluronics hydrogel can be considered as a porous semi-permeable network. This network thus permits the free flow of fluids, mainly water, and small molecules. The larger blood components such as red and white blood cells, platelets and proteins cannot enter the porous structure due to its small mesh size. This results in the development of a small osmotic pressure difference which could lead to depletion of fluid and other small molecules from the polymer network.<sup>43,44</sup>

Osmotic pressure is a colligative property of a macromolecular solution which depends only on the number of particles or molecules of the 'solute' that cannot pass through a semi-permeable membrane, thus creating a chemical potential difference. This osmotic pressure difference can be compensated by introducing charged molecules containing ionic groups. The system can be designed such that the osmotic pressure inside the network is slightly higher than outside, so that the gel is always filled with a small positive pressure.

Presence of ionic groups in the cross-linked Pluronics hydrogel is thus important to maintain osmotic balance in order to prevent excessive swelling of the gel. This can be achieved by using sodium acrylate. Hydrogels comprising of a mixture of F-127 and sodium acrylate comonomer were irradiated with UV in the presence of 0.05% w/w photo-initiator. Viscosity measurements confirmed UV radiation induced photo-polymerization of sodium acrylate as (Figure 4.11). Gels consisting of appropriate amounts of sodium acrylate can thus be photo-polymerized by UV radiation to attach ionic groups to the polymer network.

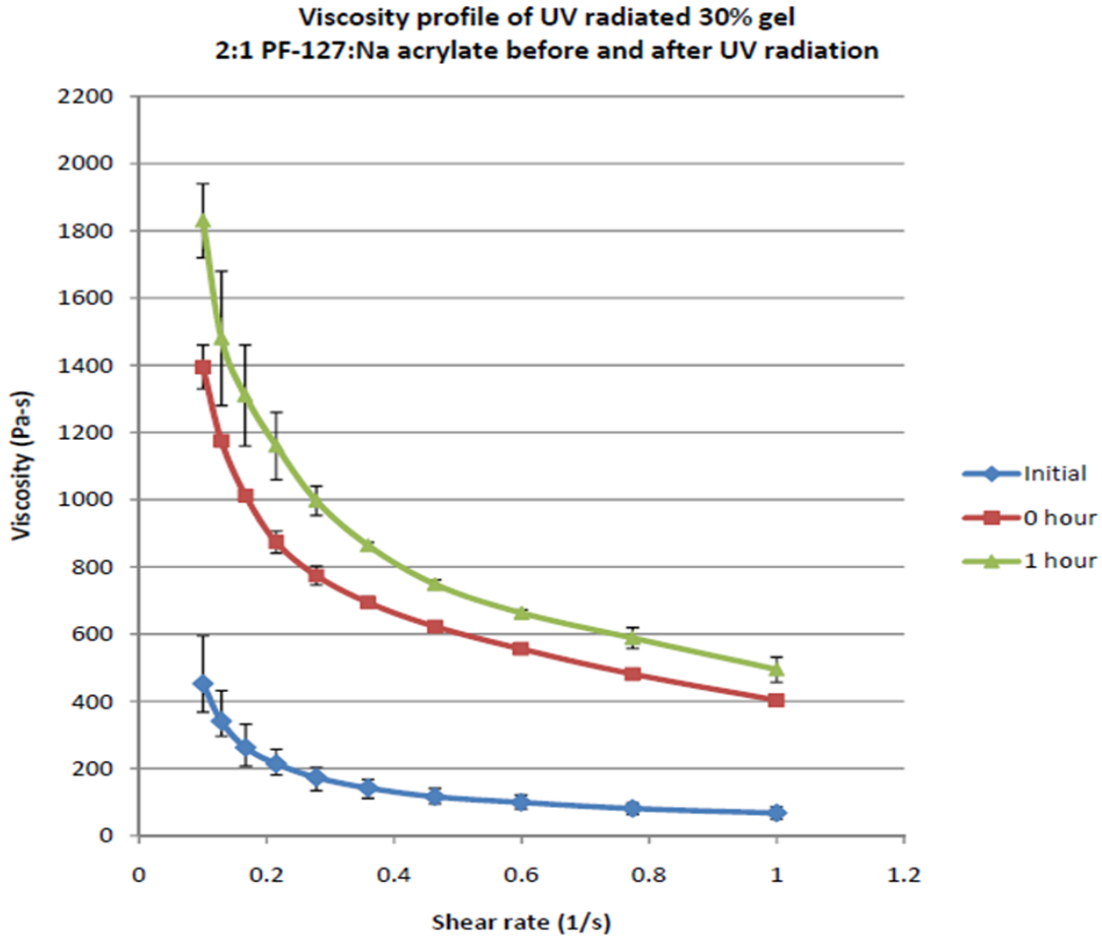


Figure 4.11: Viscosity of 30% w/w 2:1 F-127: Sodium Acrylate gel before and after UV irradiation; Initial: before UV radiation, 0 hour: after UV radiation

## 4.8 Scanning Electron Microscopy

SEM measurements were carried out to investigate the porosity of the polymer network. The images obtained from the SEM are shown in Figure 4.12. In the first image, we can see the presence of pores in the cross-section of the polymer network. However, the number of pores is limited and the overall porosity appears to be much less to promote cell penetration and propagation. It can be seen from the second image that the size of the pores is in the order of  $\mu\text{m}$



which is suitable for cell penetration. However, Additional methods to increase porosity of the network have to be explored to promote cell growth.

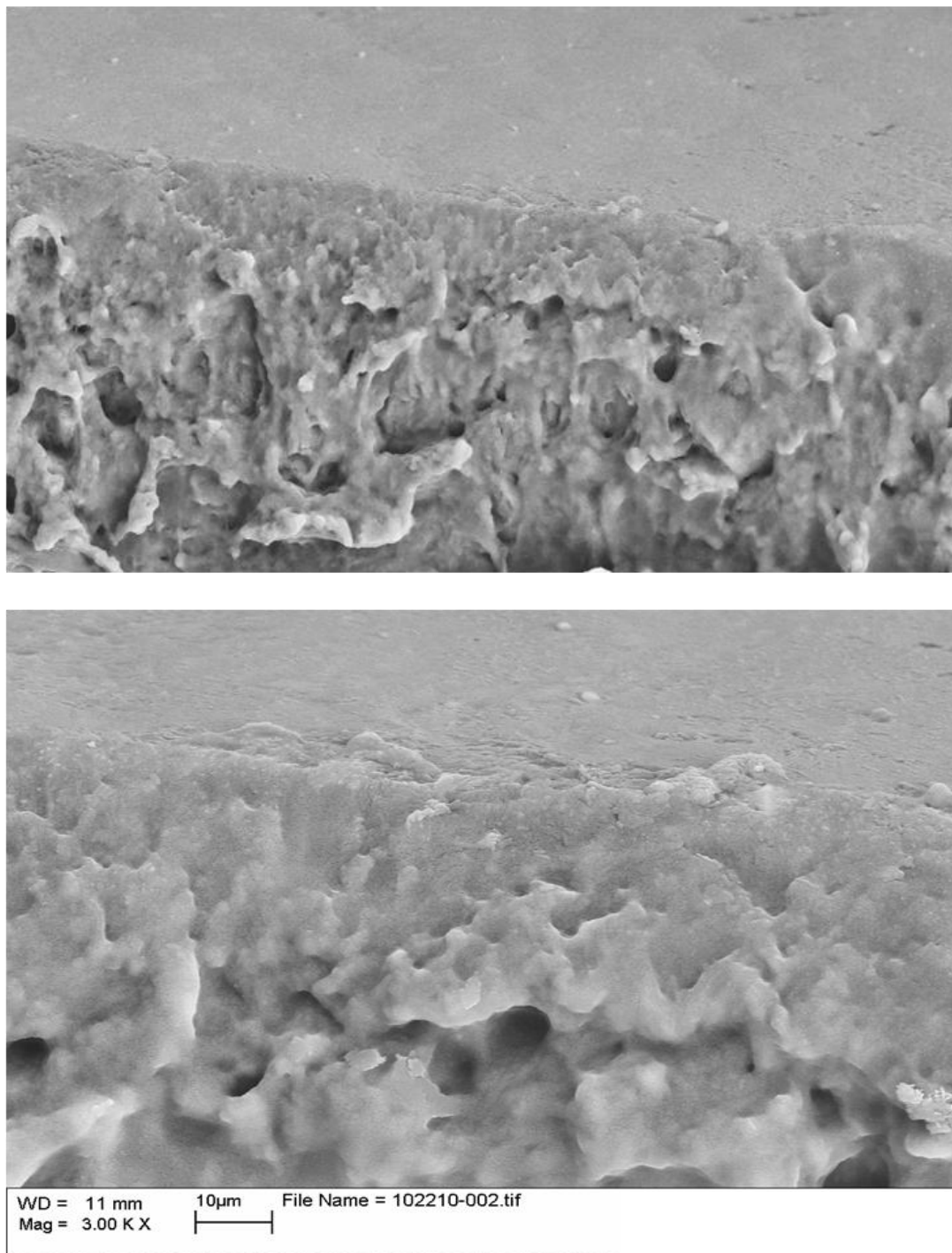


Figure 4.12: SEM images of cross-linked DA-F127 gel cross-section

## 4.9. Small Angle X-ray Scattering

Figure 4.13 shows the typical SAXS intensity patterns of all the gel samples and the corresponding radially averaged 1-D intensity profiles.

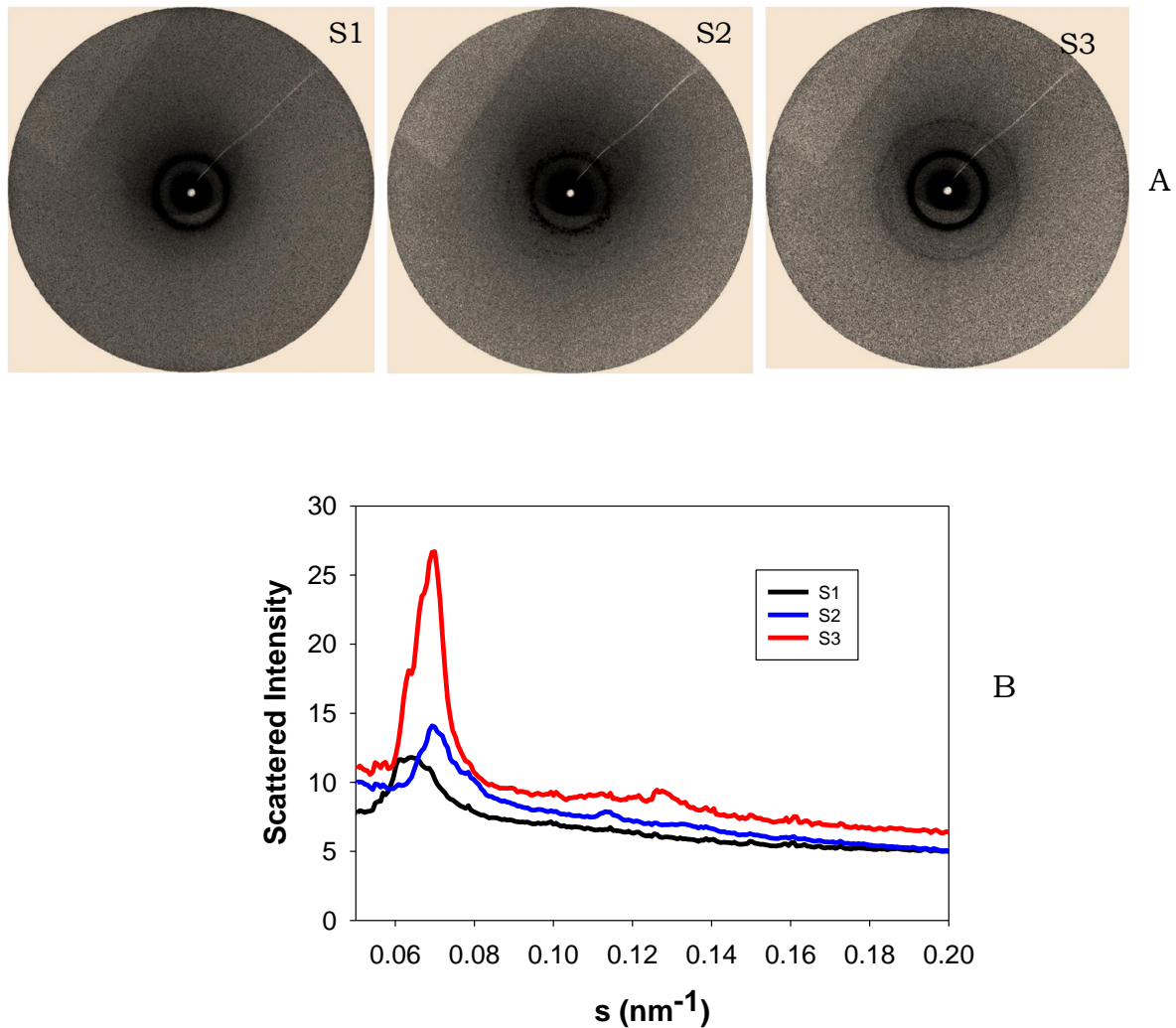


Figure 4.13 (A) Typical SAXS intensity pattern of (S1) 30% w/w 2:1 DA-F127: PEG (1.5 kDa), (S2) 20% w/w DA-F127, (S3) 30% w/w DA-F127. (B) Corresponding radially averaged 1-D intensity profile

All three samples exhibited multiple peaks, as can be seen in the radially averaged 1-D intensity profile in the figure. Thus, for every sample, peak fitting was done by using the PeakFit software to obtain the correct ratio of peak positions to determine the structure. It was determined that all the samples consisted of a mixture of hexagonal closed packing of spheres (HCPS) structure and face centered cubic (FCC) structure. The fitting curves of all the samples along with the HCPS and FCC standard peak positions are shown in Figure 4.14.

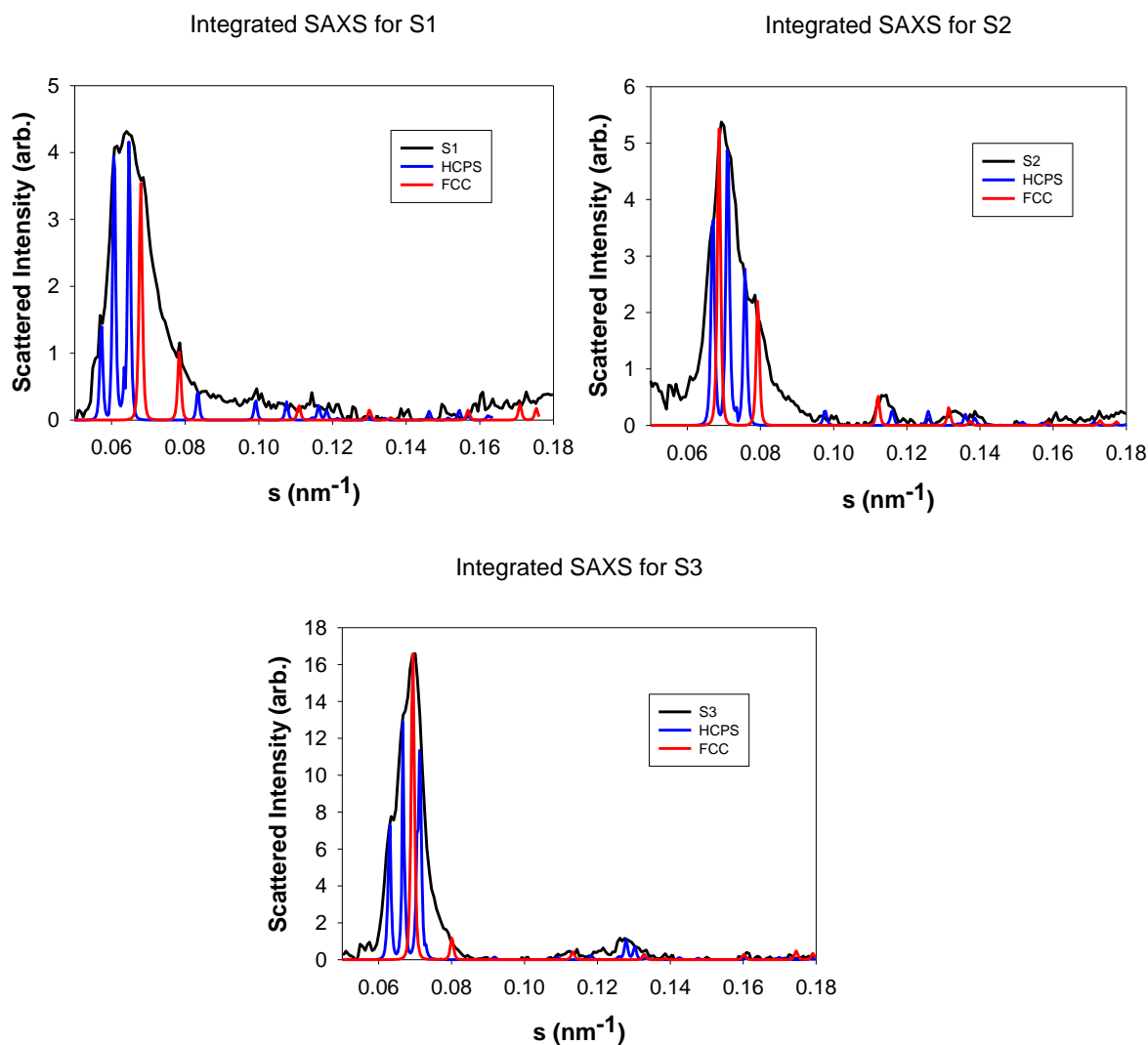


Figure 4.14: Integrated fitting curves of S1, S2 and S3

Multiple peaks were observed in all the samples. The peak positions following the mathematical relation of  $3^{1/2} : 2 : 8^{1/2} : 11^{1/2} : 12^{1/2} : 4$  is a characteristic for a FCC structure. Peak positions following the mathematical relation of  $32^{1/2} : 6 : 41^{1/2} : 68^{1/2} : 96^{1/2} : 113^{1/2} : 128^{1/2}$  is a characteristic for a HCPS structure. All the cross-linked gels were found to consist of a mixture of both FCC and HCPS structure. The ratio of FCC to HCPS in each sample was determined using the integrated areas of the fitted peaks for FCC and HCPS, respectively, to the integrated area of the sample. 30% DA-F127 gel consisted of a majority of HCPS structure (87%) and 13% FCC structure. 20% DA-F127 gel was found to have 58% FCC structure and 42% HCPS structure. The 30% w/w gel containing the polymer mixture was calculated to have approximately 69% HCPS structure and 31% FCC structure.

Gels made from pure Pluronic F-127 are known to possess FCC structure.<sup>45</sup> From the results, it appears that low polymer concentration results in a dominance of FCC structure and as the polymer concentration increases, the HCPS structure begins to dominate. The presence of PEG in sample 1 reduced the ratio of HCPS structure. This implies that the presence of PEG chains in the cross-linked network increases the extent of FCC structure.

Lattice constants were generated from fitting the integrated sample with the HCPS and FCC standard peak positions. Lattice constant 'a' gives the nearest center-to-center distance between the micelles. Sample 1 was found to have a lattice constant of 20 nm and sample 2 and 3 had lattice constant values of approximately 18 nm each. This implies that the presence of PEG does not significantly alter the lattice constant. Also, the 20% and 30% w/w concentrations of DA-F127 resulted in the same values of the lattice constant.

# Chapter 5

## Conclusion and Future Work

Multiple aspects of this polymer network can be examined and improved in the future experiments. Important aspects include increasing porosity of the network and conducting studies to characterize the pore size, and modifying the surface of the hydrogel to enable cell adhesion.

### **5.1 Formation of porous network**

A substantial amount of scaffold porosity is required to obtain homogeneous cell distribution and interconnection in the scaffold. Scaffolds should thus possess a high degree of porosity to allow cells to migrate into the scaffold to assist in vascularization and structural integration with the surrounding tissue. Optimum pore size for fibroblast in-growth is reported to be 5-15  $\mu\text{m}$ . The scaffold should thus have some fractions of connected pore size in the order of few microns to enable cell attachment and penetration. Porosity also results in enhanced diffusion and transport of nutrients and oxygen, especially in the absence of a functional vascular system. Several methods have been reported in the literature to obtain porosity in tissue engineering scaffolds. Salt leaching, freeze drying, gas foaming are some of the techniques used

to obtain pores in a polymer network. These techniques can be explored to create larger pores in the DA-F127 polymer network.

In the salt/particle leaching technique, a porogen of known particle size is dispersed in the polymer solution. Once the polymer network is formed, the particles are leached or dissolved by immersing the network in a selective solvent. Based on the end application and the type of hydrogel, a variety of porogens can be used for this application. Salt leaching is one of the most popular techniques used, since they are inexpensive, easy to handle and stable under diverse processing conditions. The nature of the porogen used has been found to play an important role in pores interconnectivity. Porogen geometry has an effect on the structure of the porous network and it has been proven that spherical particles result in higher interconnectivity when compared to cubic particles.<sup>46</sup> Ability to tune the pore size and overall porosity by varying the particle size and concentration of the porogen is one of the major advantages of the leaching technique. Also, the process is relatively simple and easy to experiment on a small scale. However, this method does not provide control over the orientation and the degree of interconnectivity in the pores, which is a major drawback.

Gas foaming technique relies on the principle of nucleation and growth of gas bubbles resulting in the formation of gas pockets in the gel, followed by removal of the gas, thus forming a porous structure. The gas bubbles can be formed by a foaming agent via a chemical reaction or can be released from a pre-saturated gas-polymer mixture at high pressure. Foaming agent is a substance which generates a gas upon chemical decomposition. Foaming agent such as sodium bicarbonate can be used due to its ability to generate CO<sub>2</sub> in slightly acidic conditions. Pore sizes ranging from 100 – 250 μm can be obtained by this method, which is sufficient to allow cellular invasion and proliferation. This size range is fairly large and only a small fraction of the void

volume should possess such pore sizes. Several inexpensive foaming agents are available for this technique. These agents are usually cell friendly and the technique does not require the use of any organic solvents, thus making it a good approach to obtain a porous network. However, this method is not known to provide good pore interconnectivity which is a drawback.<sup>47,48</sup>

The above described techniques have several advantages and disadvantages. They can be studied in detail and a suitable approach may then be devised to create an interconnected porous polymer network.

## **5.2 Structural Studies**

SAXS experiments on the cross-linked polymer network indicated that the presence of PEG does not significantly increase the distance between micelles (lattice constant). However, the studies were performed on non-swollen gel samples. SAXS experiments on swollen, equilibrated gel samples can be performed to obtain the lattice constant values of the equilibrated samples.

Structural studies provide valuable information about the shape and microstructure of the network and also some aspects of the pore size distribution. These results can then be used to engineer methods to modify the porosity of the polymer network to favor cell penetration and cell proliferation.

## 5.3 Modification of Surface Properties for Cell Adhesion

As reported in the results section, the polymer network did not facilitate cell attachment or cell adhesion on the surface of the hydrogel. Adhesion of cells to the polymer network is important for the growth of cells in culture. Adhesion occurs as a result of receptor-ligand interaction and depends on the physicochemical properties of the interacting surface molecules. Interaction occurs between the cell surface receptors and the ligands for these receptors on the surface of the polymer scaffold, as a result of specific recognition by the cell surface adhesion receptors.<sup>49</sup>

Cell adhesion to the surface of the polymer network thus is favored by the inclusion of cell adhesion peptides in the network. The degree of cell adhesion will depend on the amount of peptide grafted onto the polymer structure. Appropriate ligands should be chosen for this purpose since the cell adhesive receptors need to interact with the ligands to enable cell adhesion. The cell adhesion can thereby, generate forces required for cell migration and secrete enzymes to create pathways for cell migration through the network.<sup>50</sup>



## 5.4 Conclusion

The project is very promising since the cross-linked hydrogel exhibits the desired mechanical properties to function as an implant in the breast tissue. The cross-linked hydrogel and its various constituents are also proven to be non-toxic and thus will not result in any undesirable immune response in the human body. The presence of both hydrophobic and hydrophilic moieties in the polymer allows incorporation of additional drugs and other agents required by the scaffold.

Clinical goals for breast tissue engineering include the formation of a regenerated tissue that both cosmetically and mechanically resemble the native tissue. The mechanical integrity, sustainability and viability of the tissue over time are important concerns. Ability to deliver nutrients and oxygen by other mechanisms, in addition to diffusion as well as improvements in the long term sustainability of the engineered tissue would significantly enhance the potential of tissue constructs.

If successful, this polymer network can be used for a variety of other applications as well. These include, targeted drug delivery, sustained drug release and implants for other post-operative cancer patients.

# Bibliography

<sup>1</sup>Veronesi, U.; Cascinelli, N.; Mariani, L.; Greco, M.; Saccozzi, R.; Luini, A.; Aguilar, M.; Marubini, E., Twenty-year follow-up of a randomized study comparing breast-conserving surgery with radical mastectomy for early breast cancer. *N Engl J Med* 2002, 347 (16), 1227-32

<sup>2</sup> Lazovich D.A.; White E.; Thomas D.B.; Moe R.E., Underutilization of breast-conserving surgery and radiation therapy among women with stage I or II breast cancer. *J American Medical Association* 1991, 266, 3433-38

<sup>3</sup> Veronesi U.; Marubini E.; Mariani L.; Galimberti V.; Luini A.; Veronesi P.; Salvadori B.; Zucali R, Radiotherapy after breast-conserving surgery in small breast carcinoma: Long-term results of a randomized trial. *Annals of Oncology* 2001, 12, 997-1003

<sup>4</sup> Waljee J. F.; Hu, E. S.; Ubel, P. A.; Smith, D. M.; Newman, L. A.; Alderman, A. K., Effect of esthetic outcome after breast-conserving surgery on psychosocial functioning and quality of life. *J Clin Oncol* 2008, 26 (20), 3331-7

<sup>5</sup> Patrick C.W. Jr, Breast tissue engineering. *Annu. Rev. Biomed. Eng.* 2004, 6, 109-30

<sup>6</sup> Rozen W.M.; Rajkomar A.K.S.; Anavekar N.S.; Ashton M.W., Post-Mastectomy breast reconstruction: A history in evolution. *Clinical Breast Cancer* 2009, 9(3), 145-54

<sup>7</sup> Brown J.B.; Fryer M.P.; Ohlweiler M.P., Study and use of synthetic materials, such as silicones and teflon, as subcutaneous prostheses. *Plast Reconstr Surg* 1960, 26, 264-79

<sup>8</sup> Sanchez G.J.; Colditz G.A.; Karlson E.W.; Hunter D.J.; Speizer F.E.; Liang M.H., Silicone breast implants and the risk of connective-tissue diseases and symptoms. *N Engl J Med* 1995, 1666-70

<sup>9</sup> Grodzinski J.J., Polymeric gels and hydrogels for biomedical and pharmaceutical applications. *Polym. Adv. Technol.* 2010, 21, 27-47

<sup>10</sup> Peppas N.A.; Bures P.; Leobandung W.; Ichikawa H., Hydrogels in pharmaceutical formulations. *Eur J Pharm Biopharm.* 2000, 50, 27-46

<sup>11</sup> Hoffman A.S., Hydrogels for biomedical applications. *Advanced Drug Delivery Reviews* 2002, 43, 3–12

<sup>12</sup> Chu B., Structure and dynamics of block copolymer colloids. *Langmuir* 1996, 11, 414-421

<sup>13</sup> Batrakova E.V.; Kabanov A.V., Pluronic block copolymers: Evolution of drug delivery concept from inter nanocarriers to biological response modifiers. *Journal of Controlled Release* 2008, 130(2), 98-106.

<sup>14</sup> Liu T.; Xie Y.; Chu B., Use of block copolymer micelles on formation of hollow MoO<sub>3</sub> nanospheres. *Langmuir* 2000, 16, 9015-22

- <sup>15</sup> Loh W., Block copolymer micelles. Encyclopedia of Surface and Colloid Science: Second Edition 2006, 1014-1025
- <sup>16</sup> Wu C.; Liu T.; Chu B., Characterization of the PEO-PPO-PEO triblock copolymer and its application as a separation medium in capillary electrophoresis. Macromolecules 1997, 30, 4574-83
- <sup>17</sup> Liu T.; Burger C.; Chu B., Nanofabrication in polymer matrices. Progress in Polymer Science 2003, 28, 5-26
- <sup>18</sup> Ulanski P.; Pawlowska W.; Kadlubowski S.; Henke A.; Gottlieb R.; Arndt K.F.; Bromberg L.; Hatton T. A.; Rosiak J. M., Synthesis of hydrogels by radiation-induced crosslinking of Pluronic (R) F127 in N<sub>2</sub>O-saturated aqueous solution. Polym. Adv. Technol 2006, 17 (9-10), 804-813
- <sup>19</sup> Kabanov A.V.; Batrakova E.V.; Alakhov V.Y., Pluronic (R) block copolymers as novel polymer therapeutics for drug and gene delivery. Journal of Controlled Release 2002, 82 (2-3), 189-212
- <sup>20</sup> Bohorquez M.; Koch C.; Trygstad T.; Pandit N., A study of temperature dependent micellization of pluronic F-127. J Colloid Interface Sci. 1999, 216, 34-40
- <sup>21</sup> Yoo H. S., Photo-cross-linkable and thermo-responsive hydrogels containing chitosan and Pluronic for sustained release of human growth hormone (hGH). J Biomat. Sci, Poly. Ed. 2007, 18 (11), 1429-1441

- <sup>22</sup> Liu T.; Burger C.; Chu B., Nanofabrication in polymer matrices. *Prog. Polym. Sci.* 2003, 28, 5–26
- <sup>23</sup> Chavez C.J.J.; Cervantes L.M.; Naik A.; Kalia Y.N.; Guerrero Q. D.; Quintanar G.A., Applications of thermo-reversible pluronic F-127 gels in pharmaceutical formulations. *J Pharm Pharma Sci.* 2006, 9 (3), 339-58
- <sup>24</sup> Chung H. J.; Lee Y.; Park T.G., Thermo-sensitive and biodegradable hydrogels based on stereocomplexed Pluronic multi-block copolymers for controlled protein delivery. *J Controlled Release* 2008, 127 (1), 22-30
- <sup>25</sup> Lee J. B.; Yoon J. J.; Lee D. S.; Park T. G., Photo-crosslinkable, thermo-sensitive and biodegradable Pluronic hydrogels for sustained release of protein. *J Biomat. Sci, Poly. Ed.* 2004, 15 (12), 1571-1583.
- <sup>26</sup> Patel P.N.; Smith C.K.; Patrick, Jr C.W.; Rheological and recovery properties of poly(ethylene glycol) diacrylate hydrogels and human adipose tissue. *J Biomed Mat Res PartA* 2005, 73A(3), 313-319
- <sup>27</sup> Eiselt P.; Yeh J.; Latvala R.K.; Shea L.D.; Mooney D.J., Porous carriers for biomedical applications based on alginate hydrogels. *Biomaterials* 2000, 21, 1921-27
- <sup>28</sup> Green H, Meuth M. An established pre-adipose cell line and its differentiation in culture. *Cell* 1974, 3, 127-133

- <sup>29</sup> Freshney I.R., Culture of animal cells: A manual of basic technique and specialized applications, 2010
- <sup>30</sup> Clough R. L., High-energy radiation and polymers: A review of commercial processes and emerging applications. Nuclear instruments and methods in physics research section B-Beam interactions with materials and atoms 2001, 185, 8-33
- <sup>31</sup> Niibe Y.; Kuranami M.; Matsunaga K.; Takaya M.; Kakita S.; Hara T.; Sekiguchi K.; Watanabe M.; Hayakawa K., Value of high-dose radiation therapy for isolated osseous metastasis in breast cancer in terms of oligo-recurrence. Anticancer Res 2008, 28 (6B), 3929-31
- <sup>32</sup> Lee, S. Y.; Tae, G.; Kim, Y. H., Thermal gellation and photo-polymerization of diacrylated Pluronic F 127. J. Biomat. Sci. Pol. Ed. 2007, 18 (10), 1335-1353
- <sup>33</sup> Lee, S. Y.; Tae, G., Formulation and in vitro characterization of an in situ gelable, photopolymerizable Pluronic hydrogel suitable for injection. Journal of Controlled Release 2007, 119 (3), 313-319
- <sup>34</sup> Park H; Guo X; Temenoff J.S.; Tabata Y; Caplan A.I.; Kasper F.K.; Mikos A.G., Effect of swelling ratio of injectable hydrogel composites on chondrogenic differentiation of encapsulated rabbit marrow mesenchymal stem cells in vitro. Biomacromolecules, 2009, 10(3), 541-6
- <sup>35</sup> Devi U.C.; Sreekumari R.B.C.; Vasu R.M., Measurement of visco-elastic properties of breast –tissue mimicking materials using diffusive wave spectroscopy. J. Biomed. Opt. 2007, 12 (3)

- <sup>36</sup> Patel P. N.; Gobin A.S.;Jennifer L. W.; Patrick C.W., Poly(ethylene glycol) hydrogel system supports preadipocyte viability, adhesion, and proliferation. *Tissue Engineering, Journal of Biomedical Materials Research Part A*, 2005, 73 (3), 313-31
- <sup>37</sup> Patrick C.W.Jr.; Chauvin P.B.; Hobley J.; Reece G.P., Preadipocyte seeded PLGA scaffolds for adipose tissue engineering. *Tissue Engineering* 1999, 5(2), 139-50
- <sup>38</sup> Berridge, M.V.;Tan A.S., Characterization of the cellular reduction of 3-(4,5-dimethylthiazol-2-yl)-2,5-diphenyltetrazolium bromide (MTT): Subcellular localization, substrate dependence, and involvement of mitochondrial electron transport in MTT reduction. *Arch. Biochem. Biophys.* 1993, 303, 474–82.
- <sup>39</sup> Cory A.H.; Owen T.C.; Barltrop J.A.; Cory J.G., Use of an aqueous soluble tetrazolium/formazan assay for cell growth assays in culture. *Cancer Communications* 1991, 3(7), 208-12.
- <sup>40</sup> Molecular Probes, Live/Dead viability/cytotoxicity kit (L-3224) for animal cells, 2001
- <sup>41</sup> Patel P.N.; Smith C.K; Patrick C.W.Jr., Rheological and recovery properties of poly(ethylene glycol) diacrylate hydrogels and human adipose tissue. *J Biomed Mater Res A*. 2005, 73, 313-19
- <sup>42</sup> JR Tennant, Evaluation of the trypan blue technique for determination of cell viability. *Transplantation* 1964, 2(6), 685
- <sup>43</sup> Menke H; Grubmeyer H; Biemer E; Olbrisch R R., PVP breast implants after two years: initial results of a prospective study. *Aesthetic plastic surgery* 2001, 25(4), 278-82

- <sup>44</sup> Hayes, et al, Rheologically modified and osmotically balanced fill material for implant. 1997, US Patent : 5997574
- <sup>45</sup> Zhang J.; Gassmann M.; Chen X.; Burger C.; Rong L.; Ying Q.; Chu B., Characterization of a reversible thermoresponsive gel and its application to oligonucleotide separation. *Macromolecules* 2007, 40, 5537-44
- <sup>46</sup> Chiu Y.C.; Larson J.C.; Isom A. Jr.; Brey E.M., Generation of porous poly(ethylene glycol) hydrogels by salt leaching. *Tissue Engineering Part C* 2010, 0(0), 1-8
- <sup>47</sup> Annabi N.; Nichol J.W.; Zhong X.; Ji C.; Koshy S.; Khademhosseini A.; Deghani F., Controlling the porosity and microarchitecture of hydrogels for tissue engineering. *Tissue Engineering Part B* 2010, 16(4), 371- 83
- <sup>48</sup> Eiselt P.; Yeh J.; Latvala R.K.; Shea L.D.; Mooney D.J., Porous carriers for biomedical applications based on alginate hydrogels. *Biomaterials* 2000, 21, 1921-27
- <sup>49</sup> Dobkowski J.; Kolos R.; Kaminski J.; Kowalczyński H.M., Cell adhesion to polymeric surfaces: Experimental study and simple theoretical approach. *J. Biomat. Res.* 1999, 47(2), 234- 42
- <sup>50</sup> Mann B.K.; Gobin A.S.; Tsai A.T.; Schmedlen R.H.; West J.L.; Smooth muscle cell growth in photopolymerized hydrogels with cell adhesive and proteolytically degradable domain: synthetic ECM analogs for tissue engineering. *Biomaterials* 2001, 22, 3045-51